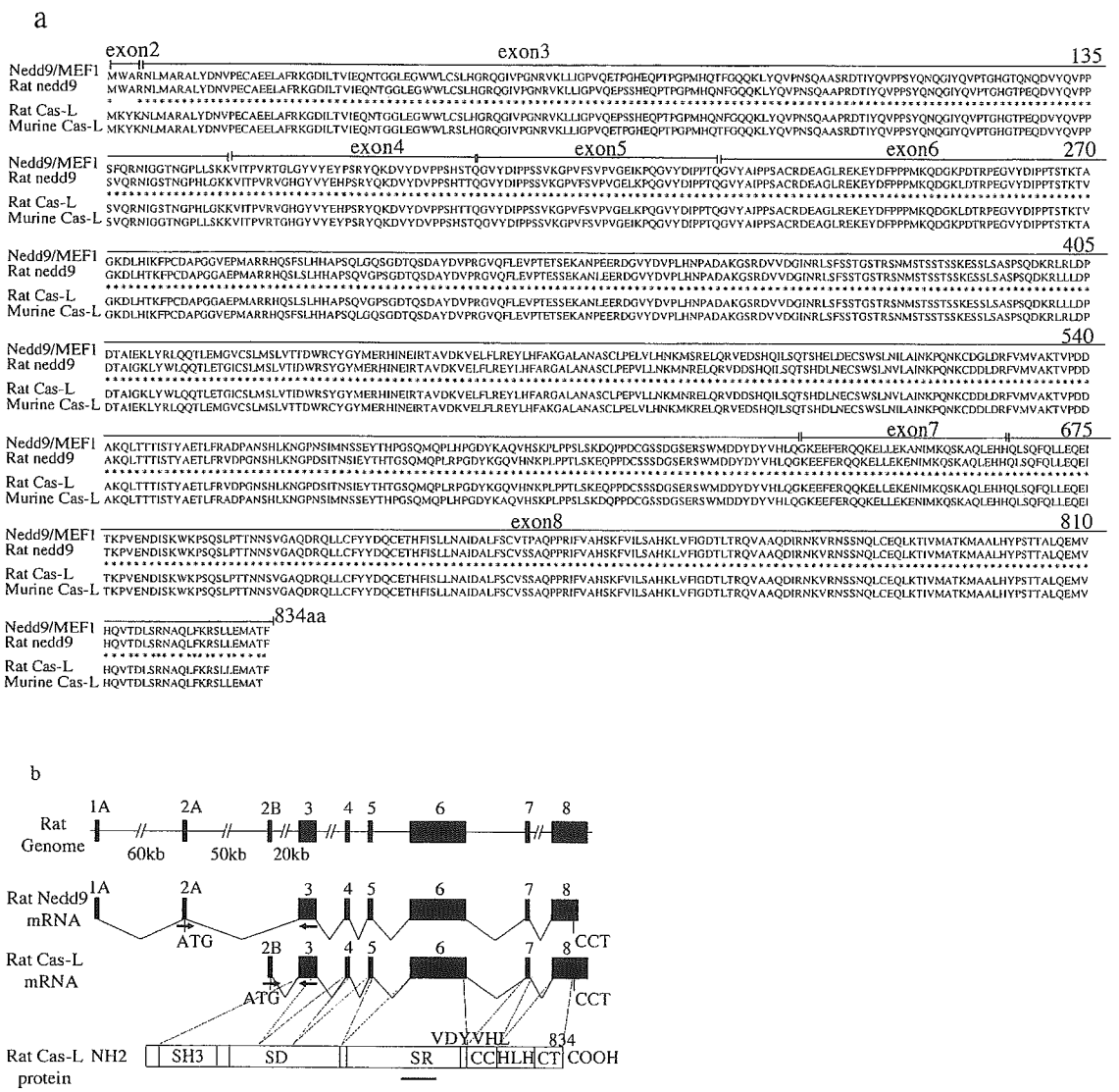

Figure 1. Nedd9 is a splicing variant of Cas-L. a, Comparison of the deduced amino acid sequences of Nedd9 and Cas-L from mouse and rat. b, Proposed model for the generation of Nedd9 and Cas-L mRNA variants and the multiple domain structure of Cas-L/Nedd9. Top, Organization of the Cas-L/Nedd9 gene. Exons are indicated by black boxes and numbered. Middle, The presence of exons in the different mRNAs represented by boxes linked by connecting lines. Translation initiation sites in exons 2A and 2B and the translation stop site in exon 8 are indicated. Arrows indicate the primer sites for PCR amplification designed to give products from Nedd9 mRNA and Cas-L mRNA, respectively. Bottom, The domain structure of Cas-L/Nedd9 is demonstrated. Bar indicates the responsible domain to be recognized by anti–Cas-L antibody used in this study. CC indicates coiled-coil regions; HLH, helix-loop-helix domain; CT, COOH-terminal region.

nucleotide sequence and 93.3% in the amino acid sequence, respectively. Rat Nedd9 shared high degrees of homology with rat Cas-L, 99.8% in nucleotide sequence and 99.8% in amino acid sequence (Figure 1a and 1b).

Nedd9, Not Cas-L, Was Transcriptionally Upregulated and Tyrosine Phosphorylated, Along With FAK in Cerebral Cortex and Hippocampus After Transient Global Ischemia

The Table shows the physiological parameters just before the induction of ischemia. There were no significant differences in the parameters among the groups, demonstrating that all of the rats used in the ischemia study had no significant difference in their condition. Expression of Nedd9 and Cas-L mRNAs in rats with global ischemia was analyzed by RT-PCR at 1, 3, 5, 7, or 14 days after 21-minute ischemia or at 1 hour after the sham operation. The RT-PCR assay was performed using a set of primers that amplifies the fragments of 203 and 225 bp from rat Nedd9 mRNA and Cas-L mRNA, respectively (Figure 1b). The expression of Nedd9 mRNA

Physiological Parameters Before the Induction of Ischemia

Day of Sacrifice	pH	Pao_2, mm Hg	$Paco_2$, mm Hg
Sham operation	7.415±0.022	73.1±2.2	35.8±2.9
1 day after ischemia	7.445±0.011	84.7±3.8	38.3±3.0
3 days after ischemia	7.442±0.003	77.0±3.1	39.0±1.9
5 days after ischemia	7.409±0.014	84.9±2.4	38.9±2.6
7 days after ischemia	7.437±0.023	90.7±4.7	37.9±4.6
14 days after ischemia	7.449±0.019	84.8±6.1	40.2±1.8

Mean±SEM. Physiological parameters did not differ among rats before induction of transient global ischemia. N=5.

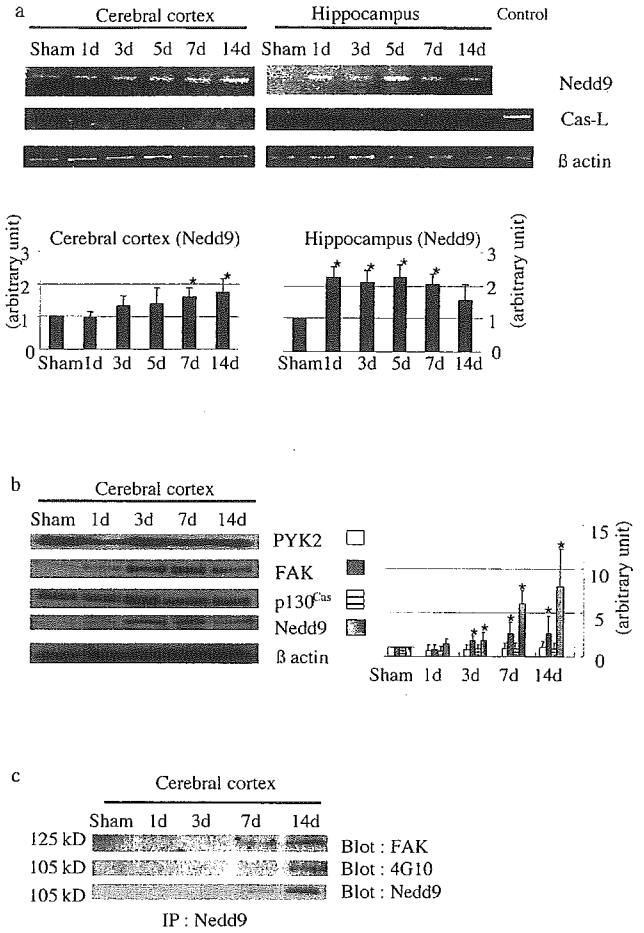

Figure 2. Nedd9 is preferentially upregulated with FAK and tyrosine-phosphorylated after transient global ischemia. a, A representative result of RT-PCR discriminating the 2 splicing variants of Cas-L/Nedd9 with β-actin as an internal control. Spleen of rats serves as positive control of Cas-L. b, The expression of proteins related to Cas-L/Nedd9 by immunoblotting. c, Nedd9 was immunoprecipitated at the indicated days after ischemia. Statistical significance is tested with respect to sham operated controls (*$P<0.001$).

was upregulated in both the cerebral cortex and hippocampus ≈1 to 14 days after ischemia, whereas the expression of Cas-L mRNA was not observed (Figure 2a).

In order to address the Cas-L/Nedd9-mediated signal transduction pathway, we examined the expression of other proteins, such as FAK, Pyk2, and p130Cas. Expression of Nedd9 protein and FAK was upregulated in a similar time course, whereas others did not show significant changes (Figure 2b). Furthermore, Nedd9 and FAK were coimmunoprecipitated at 3, 7, or 14 days after transient global ischemia. The immunoprecipitates were also blotted with the antiphosphotyrosine antibody, because activated Cas-L/Nedd9 is known to be tyrosine phosphorylated. Hence, our data demonstrated that Nedd9 was tyrosine-phosphorylated with similar kinetics as observed with protein levels of Nedd9.

Induced Nedd9 Was Localized in Dendrite-Like Structure and Cytosol of Neurons in Cerebral Cortex and Hippocampus

Nedd9- and FAK-immunoreactive cells were detected at the cerebral cortex and hippocampus 3 and 7 days after the ischemic insult but not detected at those of sham-operated rats. The expression pattern of these proteins 3 and 7 days after the ischemia were identical to each other (Figure 3a; data not shown). The rat cerebral cortex and hippocampal

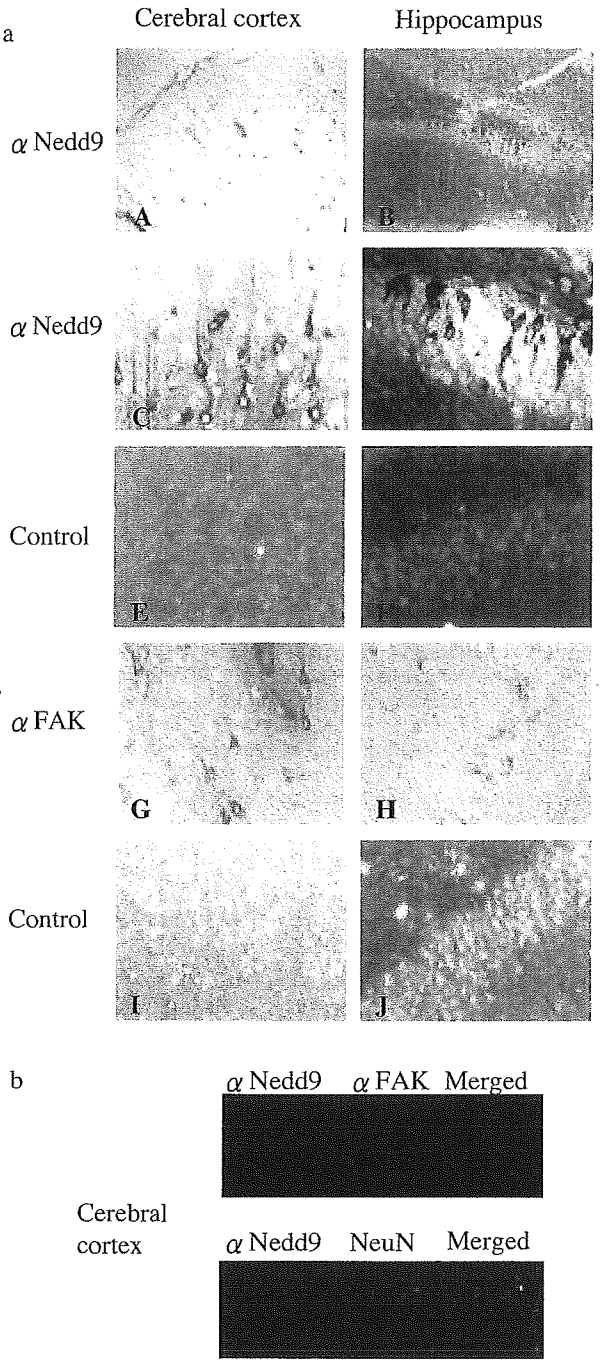

Figure 3. Induced Nedd9 protein is localized in dendrite-like structure and cytosol of neurons in the cerebral cortex and hippocampus. a, Representative figures of Nedd9 and FAK-immunoreactive cells detected at the cerebral cortex and hippocampus 7 days after transient global ischemia. Rat cerebral cortex and hippocampal coronal slices reveal intense Nedd9 and FAK immunoreactivity in the neuronal dendrites. In contrast, the neuronal cell nucleus appeared devoid of Nedd9 and FAK staining. A, C, E, G, and I, cerebral cortex; B, D, F, H, and J, hippocampus; A through D, anti-Nedd9 pAb; E and F, control; G and H, anti-FAK mAb; I and J, control; A and B, ischemia (×100); C through F and G through J, ischemia (×400); b, colocalization of Nedd9 and NeuN or FAK (×200).

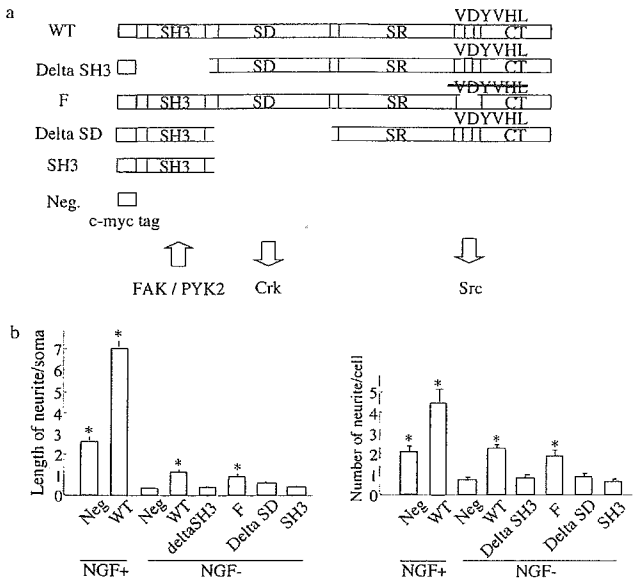

Figure 4. Nedd9 induces neurite outgrowth of PC-12 cells in the presence or absence of NGF. a, Nedd9 deletion mutants are shown. WT indicates wild type; SD, substrate domain; F, YDYVHL motif was mutated to FDFVHL; SR, serine-rich domain; CC, coiled-coil regions; HLH, helix-loop-helix domain; CT, COOH-terminal region. b, Neurite formation in the absence or presence of NGF. Data are expressed as neurite length averaged over diameter of soma (bar diagrams; *y* axis=cell diameters) and as number of neurites per cell. Statistical significance is tested with respect to unstimulated control PC-12 cells (*$P<0.001$).

coronal slices revealed intense Nedd9 immunoreactivity in the dendrite-like structures and cytosol. In contrast, the nucleus appeared devoid of Nedd9 staining. Colocalization of Nedd9 protein and FAK or NeuN confirmed the fact that Nedd9 protein was expressed in FAK-positive neurons (Figure 3b).

Nedd9 Promoted Neuronal Outgrowth of PC-12 Cells in the Presence or Absence of NGF

In order to clarify the physiological role of Nedd9, we examined the effect of Nedd9 on neurite outgrowth in PC-12 cells. Because we preliminarily found that the Nedd9 protein was expressed in neurons undergoing differentiation in the mouse embryonic neuroseptum and neurosphere (T. Sasaki, MD, PhD, unpublished data, 2003), we hypothesized that Nedd9 might play a role in neuronal differentiation. The rat pheochromocytoma PC-12 cells have been used for molecular analysis of the signaling pathways that lead to differentiation of peripheral nervous system neurons. Recently, this cell line was widely used for assays of regulatory factors expressed during central nervous system development.[18] PC-12 cells were infected with recombinant retrovirus to express myc-tagged Nedd9 and its mutants (Figure 4a). In contrast to cells infected with empty vector and mutants such as δSH3, SH3, and δSD, those expressing wild-type Nedd9 and mutant F showed promotion of neurite genesis in the presence or absence of NGF after 6 days of the addition of NGF or vehicle (Figure 4b). These findings suggest that Nedd9 may contribute to the promotion of neuronal differentiation of PC-12 cells.

Discussion

In this study, we have shown that Nedd9 is a splicing variant of Cas-L and is transcriptionally upregulated in the dendrites and cytosol of neurons in the cerebral cortex and hippocampus from 1 to 14 days after global ischemia in rats. We have also found that Nedd9 promotes neurite outgrowth of PC-12 cells. These data demonstrate that Nedd9, which is upregulated transiently during neuronal development and disappears in the adult brain, is reupregulated for neuronal differentiation after ischemia.

This is the first report to demonstrate that Cas-L and Nedd9 are splicing variants. The genetic difference between Cas-L and Nedd9 involves just 3 amino acids in the NH_2-terminus (Figure 1a): MKYK and MWAR, respectively. The fact that only Nedd9, but not Cas-L, expression is induced in response to ischemia recapitulates the physiological role of Nedd9, because it is expressed in NPCs during brain development (Figure 2a). The difference in expression between Nedd9 and Cas-L in the brain may be because of the transactivation of the Nedd9 gene mediated by nuclear factor κB, heat shock factor 1, or other related transcription factors known to be induced gradually after ischemia, because their binding sites exist in the upstream region of the rat Nedd9 gene. The molecular mechanism of Nedd9 gene regulation in these neurons will be an important subject for additional studies.

This is the first report to identify the expression of Nedd9 in the adult brain. In the focal ischemia model of mice, upregulation of several genes has been investigated and grouped as temporal episodes or "waves" of expression of different groups of genes.[1] Later waves of new gene expression, like Nedd9, include mediators that appear to be important in tissue remodeling and recovery of functions,[19] such as TGF-β[20] and osteopontin.[21] In this study, Nedd9 was selectively induced and tyrosine-phosphorylated in neurons of the cerebral cortex and hippocampus 1 to 14 days after transient global ischemia (Figures 2b and 2c and 3a and 3b). The regional difference of temporal expression of those proteins may be because of the different response to ischemic insult between the cerebral cortex and hippocampus. Those results led us to postulate that Nedd9 is required for neuronal differentiation, being primarily expressed in the embryonic brain but not in the fully differentiated adult neurons. Recently, it has been reported that stroke increases cell proliferation, with stroke-generated new neurons, as well as neuroblasts already formed before the insult, migrating into the damaged area.[22] These cells undergo differentiation and repair the neuronal network as short, remodeled neurons. The upregulation of Nedd9 in the adult brain appears to play a role in differentiation of neurons after ischemia.

To test the above hypothesis, we investigated the physiological function of Nedd9 in neurite outgrowth of PC-12 cells. We demonstrated that Nedd9 had a great impact on neurite outgrowth in the presence or absence of NGF when overexpressed in PC-12 cells. The fact that expression of δSH3, SH3, and δSD (substrate domain) inhibited neurite outgrowth is compatible with the role of the functional components of Nedd9, because Cas-L/Nedd9 bind to FAK through their SH3 domains,[6] and substrate domain is required for interaction with downstream SH2-containing proteins,

such as Crk, Nck, and SH-PTP2. Crk has been reported to induce differentiation of PC-12 in an NGF-independent manner.[23] These results, thus, confirm the hypothesis that delayed expression of Nedd9 and FAK may contribute to differentiation of neurons after ischemic injury in brain. We need to additionally investigate the role of Nedd9 in vivo, because PC-12 cells are not terminally differentiated in the setting used in the present study.

The source of Nedd9-positive neurons in ischemic brain should be investigated in future studies for its potential application to clinical treatment. It has been shown that some pathological conditions, such as ischemia, induce neurogenesis in the adult mammalian brain.[24,25] Even if Nedd9-positive neurons are derived from NPCs or have existed since the occurrence of ischemic insult, Nedd9 may be required to facilitate these regenerative or differentiating processes. The overexpression of Nedd9 may lead to a widening of the therapeutic time window for cerebral ischemia, particularly in the later phase of a stroke. In conclusion, our study may support the potential of Nedd9 for participation in the differentiation of neurons after global ischemia in rats.

Acknowledgments

This work was supported by National Institutes of Health grant AR33713; in part by grants-in-aid from the Ministry of Education, Science, and Culture and Ministry of Health, Labor and Welfare of Japan (H.O. and C.M.); and a grant from the Keio Medical Association and grants from the 21st Century COE Program of the Ministry of Education, Science and Culture of Japan to Keio University. We wish to thank Dr Toshio Kitamura for retroviral vector pMX-IRES-GFP and packaging cell line Plat-E. We appreciate the advice and expertise of Drs Kenjiro Kamiguchi, Department of Pathology at Sapporo Medical University; Mamoru Shibata, Department of Neurology; Shinnosuke Shibata, Department of Physiology at Keio University School of Medicine; and Seiji Kobayashi; as well as Akiko Souta-Kurihara. We also wish to thank Fumiki Nojima for excellent secretarial assistance.

References

1. Barone FC, Feuerstein GZ. Inflammatory mediators and stroke: new opportunities for novel therapeutics. *J Cereb Blood Flow Metab.* 1999; 19:819–834.
2. Haas CA, Rauch U, Thon N, Merten T, Deller T. Entorhinal cortex lesion in adult rats induces the expression of the neuronal chondroitin sulfate proteoglycan neurocan in reactive astrocytes. *J Neurosci.* 1999;19: 9953–9963.
3. Kinoshita M, Tomimoto H, Kinoshita A, Kumar S, Noda M. Up-regulation of the Nedd2 gene encoding an ICE/Ced-3-like cysteine protease in the gerbil brain after transient global ischemia. *J Cereb Blood Flow Metab.* 1997;17:507–514.
4. Yamada K, Goto S, Oyama T, Inoue N, Nagahiro S, Ushio Y. In vivo induction of the growth associated protein GAP43/B-50 in rat astrocytes following transient middle cerebral artery occlusion. *Acta Neuropathol (Berl).* 1994;88:553–557.
5. Kumar S, Tomooka Y, Noda M. Identification of a set of genes with developmentally down-regulated expression in the mouse brain. *Biochem Biophys Res Commun.* 1992;185:1155–1161.
6. Law SF, Estojak J, Wang B, Mysliwiec T, Kruh G, Golemis EA. Human enhancer of filamentation 1, a novel p130cas-like docking protein, associates with focal adhesion kinase and induces pseudohyphal growth in Saccharomyces cerevisiae. *Mol Cell Biol.* 1996;16:3327–3337.
7. Minegishi M, Tachibana K, Sato T, Iwata S, Nojima Y, Morimoto C. Structure and function of Cas-L, a 105-kD Crk-associated substrate-related protein that is involved in beta 1 integrin-mediated signaling in lymphocytes. *J Exp Med.* 1996;184:1365–1375.
8. Kamiguchi K, Tachibana K, Iwata S, Ohashi Y, Morimoto C. Cas-L is required for beta 1 integrin-mediated costimulation in human T cells. *J Immunol.* 1999;163:563–568.
9. Ohashi Y, Iwata S, Kamiguchi K, Morimoto C. Tyrosine phosphorylation of Crk-associated substrate lymphocyte-type is a critical element in TCR- and beta 1 integrin-induced T lymphocyte migration. *J Immunol.* 1999; 163:3727–3734.
10. Tachibana K, Urano T, Fujita H, Ohashi Y, Kamiguchi K, Iwata S, Hirai H, Morimoto C. Tyrosine phosphorylation of Crk-associated substrates by focal adhesion kinase. A putative mechanism for the integrin-mediated tyrosine phosphorylation of Crk-associated substrates. *J Biol Chem.* 1997; 272:29083–29090.
11. Reynolds AB, Kanner SB, Wang HC, Parsons JT. Stable association of activated pp60src with two tyrosine-phosphorylated cellular proteins. *Mol Cell Biol.* 1989;9:3951–3958.
12. Sakai R, Iwamatsu A, Hirano N, Ogawa S, Tanaka T, Mano H, Yazaki Y, Hirai H. A novel signaling molecule, p130, forms stable complexes in vivo with v-Crk and v-Src in a tyrosine phosphorylation-dependent manner. *EMBO J.* 1994;13:3748–3756.
13. O'Neill GM, Fashena SJ, Golemis EA. Integrin signalling: a new Cas(t) of characters enters the stage. *Trends Cell Biol.* 2000;10:111–119.
14. Ohashi Y, Tachibana K, Kamiguchi K, Fujita H, Morimoto C. T cell receptor-mediated tyrosine phosphorylation of Cas-L, a 105-kDa Crk-associated substrate-related protein, and its association of Crk and C3G. *J Biol Chem.* 1998;273:6446–6451.
15. Feinberg AP, Vogelstein B. A technique for radiolabeling DNA restriction endonuclease fragments to high specific activity. *Anal Biochem.* 1983;132:6–13.
16. Smith ML, Bendek G, Dahlgren N, Rosén I, Wieloch T, Siesjö BK. Models for studying long-term recovery following forebrain ischemia in the rat. 2. A 2-vessel occlusion model. *Acta Neurol Scand.* 1984;69: 385–401.
17. Gojo S, Kitamura S, Germeraad WT, Yoshida Y, Niwaya K, Kawachi K. Ex vivo gene transfer into myocardium using replication-defective retrovirus. *Cell Transplantation.* 1996;5:S81–S84.
18. Akamatsu W, Okano HJ, Osumi N, Inoue T, Nakamura S, Sakakibara S, Miura M, Matsuo N, Darnell RB, Okano H. Mammalian ELAV-like neuronal RNA-binding proteins HuB and HuC promote neuronal development in both the central and the peripheral nervous systems. *Proc Natl Acad Sci U S A.* 1999;96:9885–9890.
19. Read SJ, Parsons AA, Harrison DC, Philpott K, Kabnick K, O'Brien S, Clark S, Brawner M, Bates S, Gloger I, Legos JJ, Barone FC. Stroke genomics: approaches to identify, validate, and understand ischemic stroke gene expression. *J Cereb Blood Flow Metab.* 2001;21:755–778.
20. Wang X, Yue TL, White RF, Barone FC, Feuerstein GZ. Transforming growth factor-beta 1 exhibits delayed gene expression following focal cerebral ischemia. *Brain Res Bull.* 1995;36:607–609.
21. Wang X, Louden C, Yue TL, Ellison JA, Barone FC, Solleveld HA, Feuerstein GZ. Delayed expression of osteopontin after focal stroke in the rat. *J Neurosci.* 1998;18:2075–2083.
22. Arvidsson A, Collin T, Kirik D, Kokaia Z, Lindvall O. Neuronal replacement from endogenous precursors in the adult brain after stroke. *Natural Medicines.* 2002;8:963–970.
23. Tanaka S, Hattori S, Kurata T, Nagashima K, Fukui Y, Nakamura S, Matsuda M. Both the SH2 and SH3 domains of human CRK protein are required for neuronal differentiation of PC12 cells. *Mol Cell Biol.* 1993; 13:4409–4415.
24. Liu J, Solway K, Messing RO, Sharp FR. Increased neurogenesis in the dentate gyrus after transient global ischemia in gerbils. *J Neurosci.* 1998;18:7768–7778.
25. Yagita Y, Kitagawa K, Ohtsuki T, Takasawa K, Miyata T, Okano H, Hori M, Matsumoto M. Neurogenesis by progenitor cells in the ischemic adult rat hippocampus. *Stroke.* 2001;32:1890–1896.

Roxithromycin Specifically Inhibits Development of Collagen Induced Arthritis and Production of Proinflammatory Cytokines by Human T Cells and Macrophages

YASUYO URASAKI, MAMORU NORI, SATOSHI IWATA, TAKAHIRO SASAKI, OSAMU HOSONO, HIROSHI KAWASAKI, HIROTOSHI TANAKA, NAM H. DANG, EIJI IKEDA, and CHIKAO MORIMOTO

ABSTRACT. ***Objective.*** Roxithromycin (RXM) is a macrolide antibiotic that is effective in treatment of chronic lower respiratory tract diseases including diffuse panbronchiolitis and bronchial asthma. Its mechanism of action apart from its antibacterial action remains unclear. To determine the mechanism of action of RXM, we evaluated the effect of RXM on T cell functions and the inflammatory responses in mice with collagen induced arthritis (CIA).

Methods. T cell proliferation, cytokine production by T cells stimulated through CD28, CD26, or PMA with or without anti-CD3 Mab, cytokine production by macrophages stimulated with lipopolysaccharide, and transendothelial migration of T cells were analyzed in the presence or absence of various concentrations of RXM. We evaluated the effect of RXM treatment in collagen induced arthritis in mice.

Results. RXM did not affect the production of Th1-type and Th2-type cytokines, whereas it specifically inhibited production of proinflammatory cytokines such as tumor necrosis factor-α and interleukin 6 (IL-6) by T cells and macrophages. RXM inhibited T cell migration. We found that RXM treatment of mice with CIA reduced the severity of arthritis and serum level of IL-6, as well as leukocyte migration into the affected joints and destruction of bones and cartilage.

Conclusion. Our findings strongly suggest that RXM may be useful for the therapy of rheumatoid arthritis as well as other inflammatory diseases such as Crohn's disease. (J Rheumatol 2005; 32:1765–74)

Key Indexing Terms:
ROXITHROMYCIN PROINFLAMMATORY CYTOKINE T CELLS COSTIMULATION COLLAGEN INDUCED ARTHRITIS MACROPHAGES RHEUMATOID ARTHRITIS

There is increasing evidence that macrolides have a variety of biologic activities apart from their antibacterial actions[1]. Recently, low dose and longterm erythromycin treatment was shown to be effective in chronic lower respiratory tract disease, including diffuse panbronchiolitis and bronchial asthma[2,3], but the mechanism of action of this drug remains unclear. Erythromycin may have antiinflammatory properties, in addition to its antimicrobial effects. These immunomodulatory effects are reported to be the result of leukocyte activation, such as stimulation of phagocytosis[4,5], natural killer cell activity[5,6], production of superoxide anion[5], and neutrophil chemotaxis[2,7-9]. Roxithromycin (RXM), a new macrolide antibiotic, has a 14-member macrocycline ring structure resembling that of erythromycin[10]. RXM is characterized by rapid and complete absorption after oral administration, resulting in high serum concentrations[11]. *In vitro* investigation revealed that RXM modifies the function of neutrophils[12] and keratinocytes[13]. RXM also affects lymphocyte functions including proliferation induced by mitogens and purified protein derivative[14], as well as proliferation and cytokine secretion induced by mitogens[10,15].

In the initial stage of immune response, a certain antigen would be engaged by the T cell receptors, followed by

From the Division of Clinical Immunology, Advanced Clinical Research Center, Institute of Medical Science, University of Tokyo; Department of Lymphoma/Myeloma, M.D. Anderson Cancer Center, Houston, Texas, USA; and Department of Pathology, Keio University School of Medicine, Tokyo, Japan.

Supported by grants-in-aid from the Ministry of Education, Culture, Sports, Science and Technology and the Ministry of Health, Labor and Welfare of Japan.

Y. Urasaki, MS; M. Nori, MD; S. Iwata, MD; T. Sasaki, MD; O. Hosono, MD; H. Kawasaki, MD; H. Tanaka, MD, Division of Clinical Immunology, Advanced Clinical Research Center, Institute of Medical Science, University of Tokyo; N.H. Dang, MD, M.D. Anderson Cancer Center; E. Ikeda, MD, Department of Pathology, Keio University School of Medicine; C. Morimoto, MD, Division of Clinical Immunology, Advanced Clinical Research Center, Institute of Medical Science, University of Tokyo.

Address reprint requests to Dr. C. Morimoto, Division of Clinical Immunology, Advanced Clinical Research Center, Institute of Medical Science, University of Tokyo, 4-6-1 Shirokanedai, Minato-ku, Tokyo, 108-8639 Japan. E-mail: morimoto@ims.u-tokyo.ac.jp

Accepted for publication April 1, 2005.

release of various cytokines. However, this process alone is not sufficient for induction of all events that accompany T cell activation. Accumulating evidence suggests the presence of so-called costimulatory signals that occur through additional T cell surface molecules, which are independent of the CD3/T cell receptors[16]. These costimulatory signals are indispensable for full activation of T cells, which is characterized by T cell proliferation and cytokine production. Triggering of costimulatory signals therefore plays an important role in the generation of hypersensitive immune reaction. These costimulatory signals can be provided by a number of accessory molecules such as CD28/CTLA-4[17,18]. In addition, we identified CD26 as a novel costimulatory molecule that is preferentially expressed on CD4+ memory T cells[19-21] and that is speculated to be involved in the functions of effector T cells that migrate to inflammatory sites in immune mediated diseases[22].

In our study, we employed the costimulatory system of peripheral T cells *in vitro* to elucidate the immunomodulatory effect of RXM. We evaluated the therapeutic effect of RXM *in vivo* using the mouse model of rheumatoid arthritis (RA).

MATERIALS AND METHODS

Cells and reagents. Human peripheral blood mononuclear cells were isolated from healthy volunteer donors by Ficoll-Hypaque (Pharmacia Biotech, Piscataway, NJ, USA) density gradient centrifugation[19]. Unfractionated mononuclear cells were separated into an E rosette-positive (E+) population and were used as resting T cells. Monocytes were depleted by adherence to plastic plates for 24 h at 37°C followed by incubation with 5 mM L-leucine methyl ester HCl (Sigma Chemical Co., St. Louis, MO, USA) for 1 h. The monoclonal antibody (Mab) OKT3 was obtained from the American Tissue Culture Collection (ATCC; Rockville, MD, USA). Anti-CD26 (1F7) and the anti-CD28 Mab 4B10 were developed in our laboratory as described[18,19]. RXM (generously supplied by Eisai Ltd., Tokyo, Japan) was dissolved in DMSO and further diluted in the culture media consisting of RPMI-1640 and 10% fetal calf serum (FCS).

T cell proliferation assays. One hundred microliters of phosphate buffered saline containing 0.05 μg/ml of OKT3 in the presence or absence of 5 μg/ml of 1F7 (anti-CD26), or 5 μg/ml of 4B10 (anti-CD28) Mab, and incubated overnight at 4°C, as described[20]. Highly purified T cells were resuspended at 1×10^5 cells in 200 μl of RPMI-1640 medium containing 10% FCS, along with 4 different concentrations of RXM (0, 1.4, 14, and 28 μM). To assess PMA stimulation, the cell suspension supplemented with 5 ng/ml of PMA was applied into OKT3-coated wells. Cells were incubated at 37°C in a 5% CO_2 humidified atmosphere for 3 days. Cells were pulsed with 1 μCi/well of ^{3}H-thymidine (ICN Radiochemicals, Irvine, CA, USA) 8 h prior to harvest onto a glass-fiber filter (Wallac, Turku, Finland), and the incorporated radioactivity was quantified by a liquid scintillation counter (Wallac).

Cytokine production assays. Antibody-coated plates and purified T cells were prepared in the manner described above, with the exception of OKT3 concentration being 0.5 μg/ml. Cytokine production by T cells was assayed in triplicates in 96-well, flat-bottomplates as described above. After 24 h incubation, culture supernatants were subjected to ELISA [interleukin 2 (IL-2) and IL-4: Biosource International, Camarillo, CA, USA; interferon-γ (IFN-γ) and IL-5: R&D Systems, Minneapolis, MN, USA] to measure the levels of IL-2, IFN-γ, IL-4, and IL-5 as well as tumor necrosis factor-α (TNF-α) and IL-6. For TNF-α and IL-6 production by macrophages, macrophages were enriched from E-rosette-negative cells by adherence to plastic plates. Macrophages (1×10^6/ml) were suspended in 10% FCS-RPMI-1640 and stimulated with 1 μg/ml lipopolysaccharide (LPS; Sigma). After 8 h culture, supernatants were harvested and were subjected to ELISA (TNF-α and IL-6; R&D Systems). The serum levels of IL-6, TNF-α, IFN-γ, and IL-4 were also detected using an ELISA kit as described.

Assessment of cell viability. The trypan blue dye exclusion test was used to assess cell viability. In all experiments, the viability was found to be > 95% at each point measured (data not shown).

Transendothelial migration assay. Transendothelial migration activity was assessed using a kind of Boyden-chamber assay as described[23] with modifications. Human umbilical vein endothelial cells (HUVEC) obtained from ATCC were precultured to make a monolayer sheet on Transwell cell culture inserts with 3.0 μm pore size (Corning Costar, Cambridge, MA, USA) for 48 h. RXM was first dissolved in DMSO and further diluted in the assay medium consisting of RPMI-1640 and 0.6% bovine serum albumin, then added to culture plates in a final volume of 600 μl (the lower chamber) just before the migration assay. PHA-activated T cells (1×10^6 cells/well) were added to each insert in a volume of 200 μl simultaneously with the same concentration of RXM as in the corresponding culture wells (the upper chamber). Spontaneous migration (chemokinesis) assay was performed at 37°C for 8 h in the presence or absence of RXM, then harvested and counted by flow cytometry (FACS Calibur, Nippon Becton-Dickinson, Tokyo, Japan) for 1 min.

Induction of CIA. Male DBA/1J mice were purchased from Japan Charles River Breeding Laboratories (Tokyo, Japan). Bovine type II collagen (Collagen Research Center, Tokyo, Japan) was dissolved at 4 mg/ml in 0.05 M acetic acid and then emulsified with an equal volume of complete Freund's adjuvant (Difco). For the primary immunization, 100 μl of the immunogen were injected intradermally into 8-week-old mice at the tail base. After 3 weeks, the mice received the same dose of immunogen subcutaneously. Arthritis developed within 10 days of the second immunization. These mice were kept under specific pathogen-free conditions in a clean room at the Animal Research Center, Institute of Medical Science, University of Tokyo.

Assessment of CIA disease severity. After physical examination, legs were scored as follows: 0, normal; 1, erythema and mild swelling confined to the ankle joint or toes; 2, erythema and mild swelling extending from the ankle to the midfoot; 3, erythema and severe swelling extending from ankle to the metatarsal joints; 4, ankylosing deformation with joint swelling[24]. The disease score for each mouse was calculated as the sum of the scores for the 2 hind legs.

Oral roxithromycin for CIA mice. RXM was dissolved in 5% arabic gum in 0.9% NaCl, and different doses of RXM (100, 200, 400, and 800 μg) were orally given to 5 different groups comprising 8 mice in each group. The 5% arabic gum, 0.9% NaCl combination alone was also given to the control mouse group orally. RXM or 5% arabic gum in 0.9% NaCl was given orally to mice every day up to Day 14 after second immunization of type II collagen.

ELISA of cytokines and type II collagen antibody levels in CIA mice. Serum samples from CIA mice were collected on the day of the first and second immunizations and Days 7, 14, and 21 after the second immunization. IL-6, TNF-α, IL-4, and IFN-γ levels were assayed by ELISA. Type II collagen antibody levels were assayed by ELISA (Chondrex, Redmond, WA, USA). Comparison of antibody levels was performed at 490 nm optical density.

Histology. Mice were euthanized by CO_2 asphyxiation and hind paws taken from CIA mice 3 weeks after the second immunization were fixed in 10% phosphate-buffered formalin (pH 7.4), decalcified in 10% EDTA, and embedded in paraffin. Sections (4 μm) were stained with hematoxylin and eosin.

Statistical analysis. Statistical analysis was performed by the 2-tailed Student's t test for all the assays (^{3}H-thymidine incorporation assay, ELISA, and transendothelial migration assay). Statistical differences of ankle width and paw width of CIA mice were assessed by Student t test, and the disease score was evaluated by Mann-Whitney U test.

RESULTS

Effect of roxithromycin on T cell proliferation through different costimulatory pathways. As shown in Figure 1, CD3 stimulation alone resulted in the induction of low levels of T cell proliferation. Marked T cell proliferation was observed with CD3 stimulation in combination with an additional second signal, such as anti-CD26 Mab, anti-CD28 Mab, or PMA. Under these conditions, RXM did not inhibit T cell proliferation from different donors at virtually any concentration tested (1.4 to 28 μM). It should be noted that at higher concentration (28 μM), only slight inhibition of T cell proliferation was observed in certain donors.

Effect of roxithromycin on Th1-type and Th2-type cytokine production through different costimulatory pathways. As shown in Figure 2A, RXM, even at 28 μM, did not inhibit IL-2 production under all costimulatory conditions. In addition to IL-2, RXM did not show any apparent effect on the production of IFN-γ at any concentrations tested (1.4 to 28 μM; Figure 2A).

Since Th2-type CD4+ T cells may play a role in allergic disorders such as asthma[25,26], we next examined the effect of RXM on Th2-type cytokine production. As shown in Figure 2A, RXM did not inhibit IL-4 and IL-5 production under each costimulatory condition at any tested doses (1.4 to 28 μM). Our results therefore indicated that RXM did not inhibit Th1-type and Th2-type cytokine production in our experimental systems.

Effect of roxithromycin on proinflammatory cytokine production through different costimulatory pathways. We next examined the effect of RXM on the production of proinflammatory cytokines. As shown in Figure 2B, production of the proinflammatory cytokines IL-6 and TNF-α was significantly inhibited by RXM in a dose-dependent manner under each costimulatory condition. Therefore RXM inhibited proinflammatory cytokine productions by T cells stimulated by our costimulatory conditions.

Effect of RXM on proinflammatory cytokine production by macrophages. Since macrophages play a role in host defense against infection and in the local modulation of immune and inflammatory responses[27], we also examined the effect of RXM on the production of proinflammatory cytokines by macrophages. The preliminary time-course

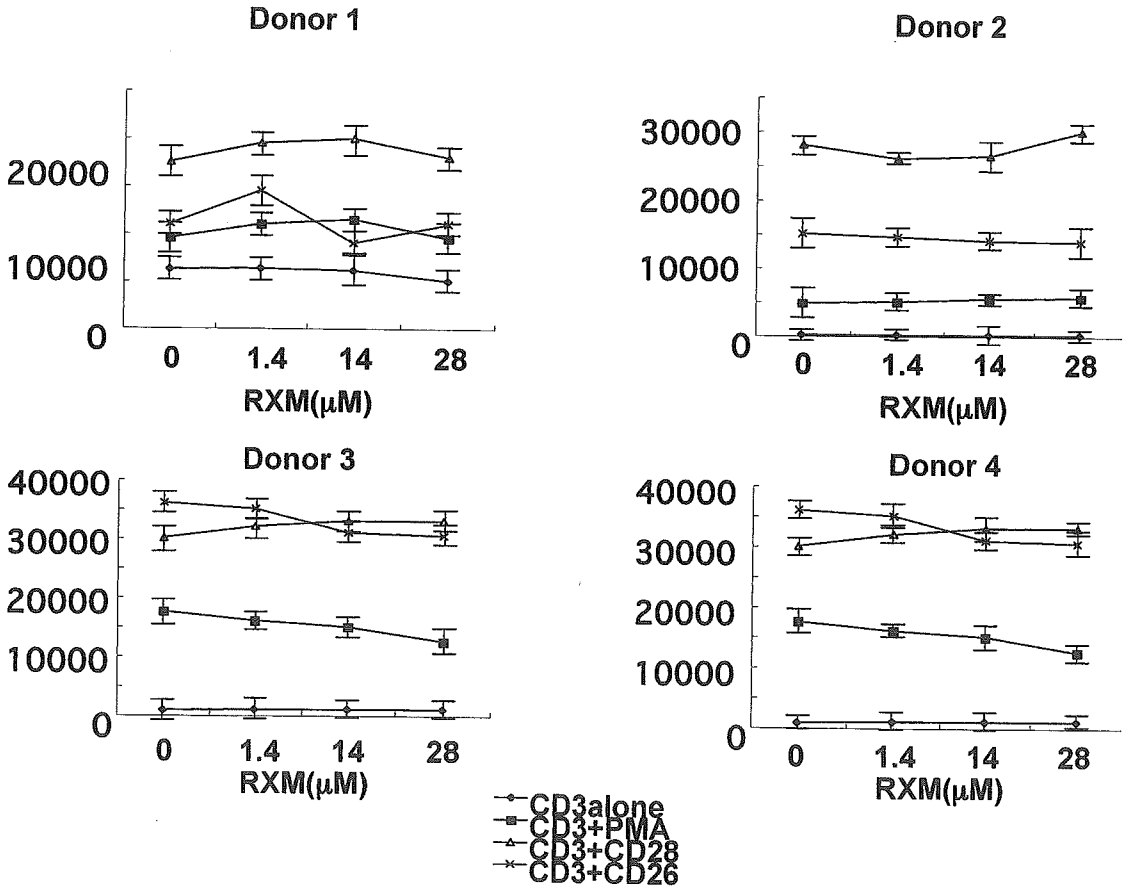

Figure 1. Effect of RXM on the proliferative response of peripheral T cells stimulated with anti-CD3 Mab alone, anti-CD3 Mab plus PMA, anti-CD3 plus anti-CD28 (4B10) Mab, and anti-CD3 plus anti-CD26 (1F7) Mab. Counts per minute (cpm) value in the case of nonstimulated T cells was near background level (data not shown). Mean cpm values ± SD from triplicate samples from 4 different donors are shown. RXM did not significantly inhibit proliferative response of T cells induced by the stimuli described above.

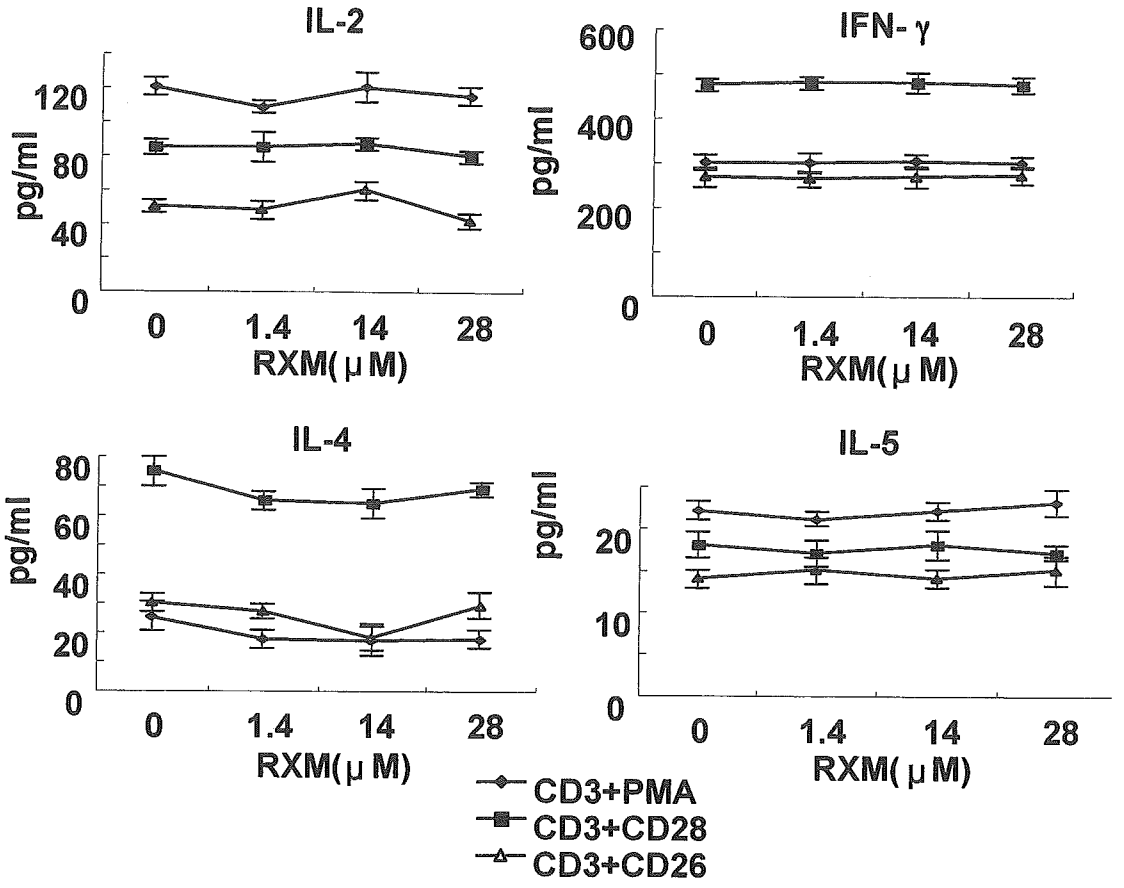

Figure 2A. Effect of RXM on peripheral T cell production of IL-2, IFN-γ, IL-4, and IL-5. T cells were stimulated with anti-CD3 plus PMA, CD3 plus CD28, and anti-CD3 plus anti-CD26 for 24 h, and culture supernatants were assayed by ELISA for cytokine levels shown here. Cytokine levels of T cells stimulated with anti-CD3 alone were always the background level (data not shown). Mean values ± SD from triplicate samples are shown; data are representative of 3 independent experiments.

experiment showed that 8 hours after stimulation was optimal for LPS-stimulated proinflammatory cytokine production by macrophages. As shown in Figure 2C, RXM inhibited both IL-6 and TNF-α production by macrophages in a dose-dependent manner.

Effect of RXM on transendothelial migration of activated T cells. We next examined its effect on transendothelial migration of PHA-stimulated T cells. These preactivated T cells spontaneously migrate from the upper chamber to the lower chamber through the endothelial monolayer, which is therefore regarded as chemokinesis. As shown in Figure 3, T cell migration was significantly inhibited in a range from 14 to 28 μM in a dose-dependent manner when RXM was present during the endothelial migration assay ($p < 0.05$). Compared to proinflammatory cytokine production by T cells and macrophages, RXM at dose of 1.4 μM did not inhibit migration of T cells from 5 different donors; but from 14 to 28 μM RXM, T cell migration was always inhibited. In contrast, when we pretreated HUVEC with various concentrations of RXM for 48 hours, and then HUVEC were washed and exposed to PHA-stimulated T cells, RXM did not affect the migration of T cells through HUVEC even at the highest concentration tested (28 μM; data not shown).

Effect of RXM therapy on the development of CIA. Finally, we investigated whether RXM affects the pathophysiology of CIA. Oral treatment of RXM was started after the second immunization of type II collagen, and daily treatment of RXM was continued up to Day 14. As shown in Figure 4, disease scores were suppressed in a dose-dependent manner after 7 days of treatment. In mice treated with RXM at a dose of 100, 200, 400, and 800 μg and control mice, statistically significant differences in disease score suppression were observed ($p < 0.05$ and $p < 0.01$). It should be noted that in the groups of mice treated with RXM 400 μg/day and 800 μg/day, disease scores were markedly inhibited, but the differences in the disease scores between the 2 groups did not reach statistical significance differences after 14 days of treatment. These results therefore indicate that RXM treatment inhibited the development of CIA.

Effect of RXM treatment on serum levels of IL-6, TNF-α, IL-4, and IFN-γ and type II collagen antibody levels. Since IL-6 and TNF-α appear to be involved in the development of

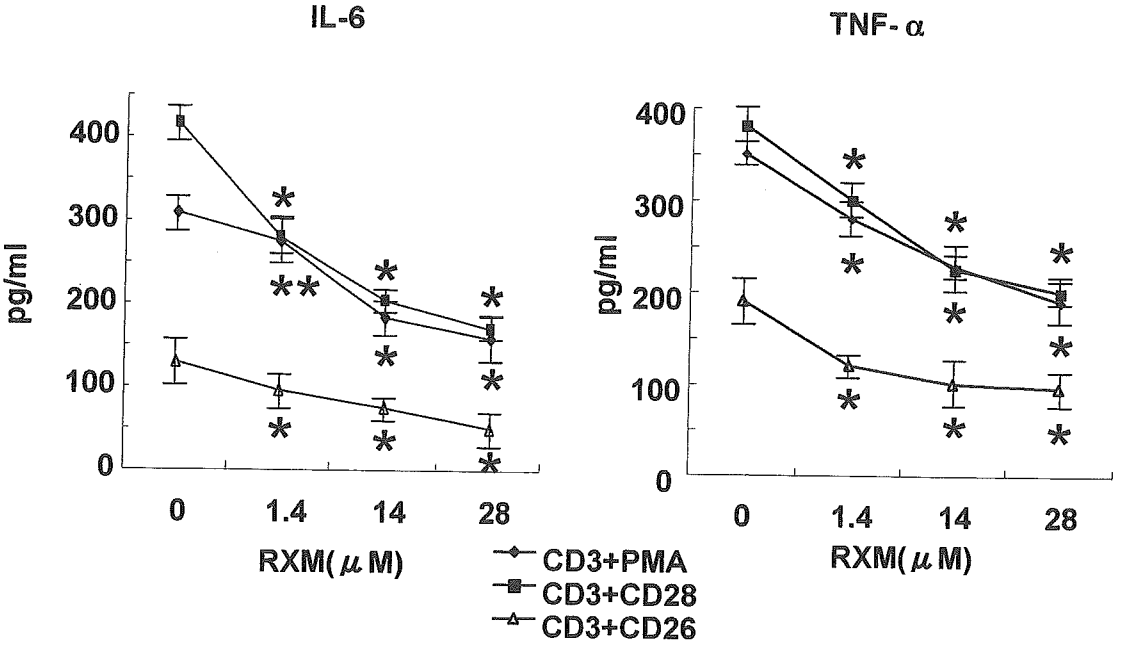

Figure 2B. Effect of RXM on peripheral T cell production of IL-6 and TNF-α. T cells were stimulated by the same conditions as in (A), and culture supernatants were assayed by ELISA for IL-6 and TNF-α. Cytokine levels of T cells stimulated with anti-CD3 alone were always the background level (data not shown). Mean values ± SD from triplicate samples are shown; data are representative of 3 independent experiments. *p <0.01, **p < 0.05 between 0 and 1.4 μM, 0 and 14 μM, 0 and 28 μM RXM; 2-tailed Student t test.

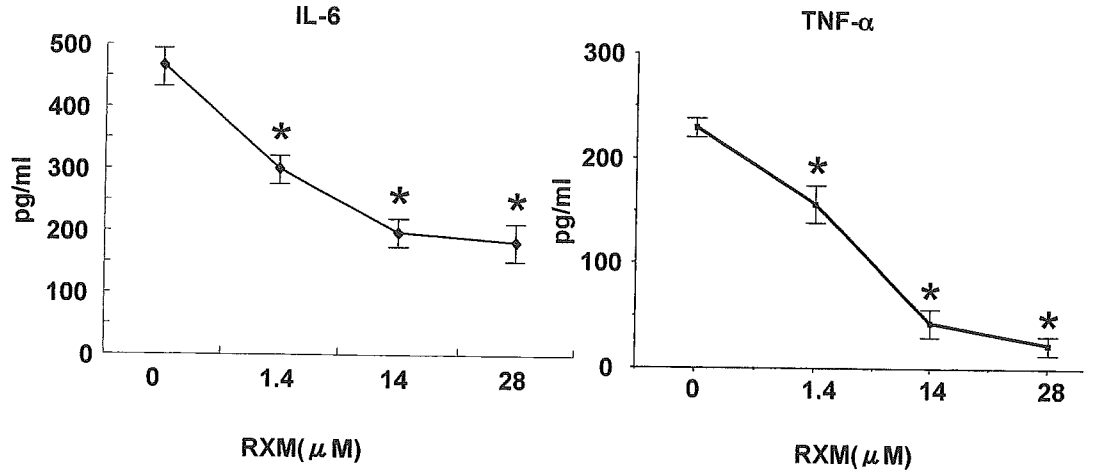

Figure 2C. Effect of RXM on production of IL-6 and TNF-α by macrophages stimulated with LPS (1 μg/ml) for 8 h; culture supernatants were assayed by ELISA for IL-6 and TNF-α. Mean values ± SD from triplicate samples are shown; data are representative of 3 independent experiments. *p <0.01 between 0 and 1.4 μM, 0 and 14 μM, 0 and 28 μM RXM; 2-tailed Student t test.

CIA[28], we examined the serum levels of those proinflammatory cytokines as well as IFN-γ and IL-4 in CIA mice on Days 0, 7, 14, and 21 after RXM treatment. While treatment of RXM did not affect the serum level of IFN-γ (Figure 5A), serum IL-6 levels increased in control CIA mice on Day 7, and then decreased to an undetectable level by Day 14. In contrast, in RXM-treated CIA mice, serum IL-6 levels were reduced on Day 7 in a dose-dependent manner. Particularly in CIA mice treated with 400 μg and 800 μg RXM, serum IL-6 levels were significantly reduced on Day 7 ($p < 0.05$; Figure 5B).

Serum IL-4 and TNF-α levels could not be detected in these groups of CIA mice due to the low degree of sensitivity of the available detection kits. Regarding type II collagen antibody levels (Figure 5C), a type II collagen antibody was detected after Day 7 of the second immunization of collagen, but RXM treatment did not affect the serum titer of this antibody. Thus we concluded that RXM treatment, particu-

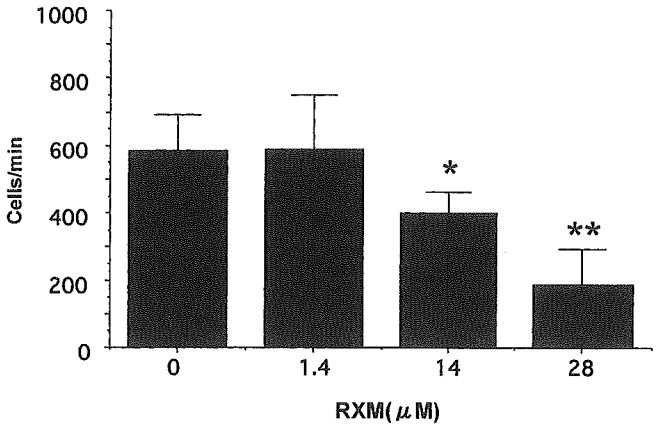

Figure 3. Inhibitory effect of RXM on transendothelial migration (chemokinesis) of PHA-activated T cells, as described in Materials and Methods. Bars show mean values ± SD of triplicate cultures. *p < 0.05 between 0 and 14 μM RXM, **p < 0.01 between 0 and 28 μM RXM; 2-tailed Student t test. Data are representative of samples from 5 different donors.

larly at the higher dose levels 400 μg and 800 μg, significantly inhibited the production of IL-6 in the serum of CIA mice.

RXM inhibition of leukocyte migration and bone destruction in affected joints of CIA mice. Histological analysis of inflamed joints and synovial tissue from those mice revealed large numbers of cells of leukocyte origin, synovial membrane proliferation, and pannus formation as well as destruction of bone and cartilage in control CIA mice not treated with RXM (Figure 6). On the other hand, in CIA mice treated with 200 and 800 μg RXM per day, the infiltration of leukocytes, cartilage and bone destruction, and pannus formation were strongly suppressed in a dose-dependent manner (Figure 6). Especially in 800 μg RXM-treated CIA mice, no cartilage and bone destruction, pannus formation, and synovial membrane proliferation was observed. These results indicated that RXM inhibited leukocyte migration as well as cartilage and bone destruction.

DISCUSSION

We demonstrated that RXM clearly inhibited the production of the proinflammatory cytokines TNF-α and IL-6 by activated T cells and macrophages. In addition, RXM inhibited T cell migration. Most importantly, RXM treatment of CIA mice inhibited the development of CIA, serum IL-6 levels, the migration of leukocytes into affected joints, and the destruction of bone and cartilage.

Previous studies showed that RXM could not inhibit concanavalin A (ConA)-induced T cell proliferation, but could inhibit ConA-induced IL-2 and IL-4 production by T cells[15]. Moreover, the same investigators reported that RXM inhibited production of Th2-type cytokine IL-4 and IL-5 but not Th1-type cytokine IL-2 and IFN-γ by T cells stimulated with the same costimulatory stimuli used in our study[29]. Although the precise reasons for the discrepancy between our findings and their data are unclear, it may be due to differences in the methods used for stimulation. Moreover, other researchers reported that other macrolides such as midecamycin, clarithromycin, and josamycin inhibited production of both Th1-type and Th2-type cytokines, such as IL-2, IL-4, and IL-5, by ConA-stimulated T cells[30]. Meanwhile, erythromycin and RXM inhibited TNF-α pro-

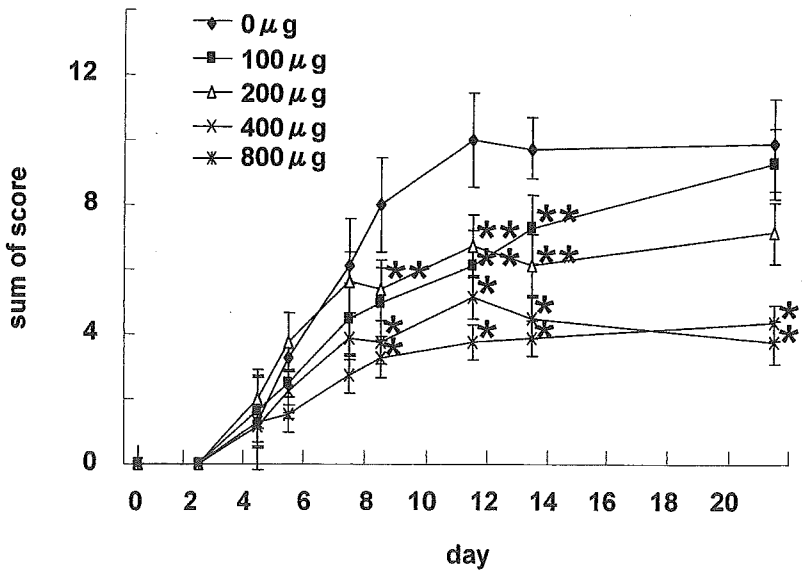

Figure 4. Effect of RXM therapy on development of CIA. Disease scores of CIA mice measured from Day 0 to Day 21 after the second immunization. Sums of scores are shown for 4 different doses of RXM (100, 200, 400, 800 μg; n = 8 for each group) and control group (n = 8). Mean values ± SD from 8 mice are plotted. *p < 0.01, **p < 0.05 between 0 and 100, 200, 400, 800 μg/day; 2-tailed Student t test.

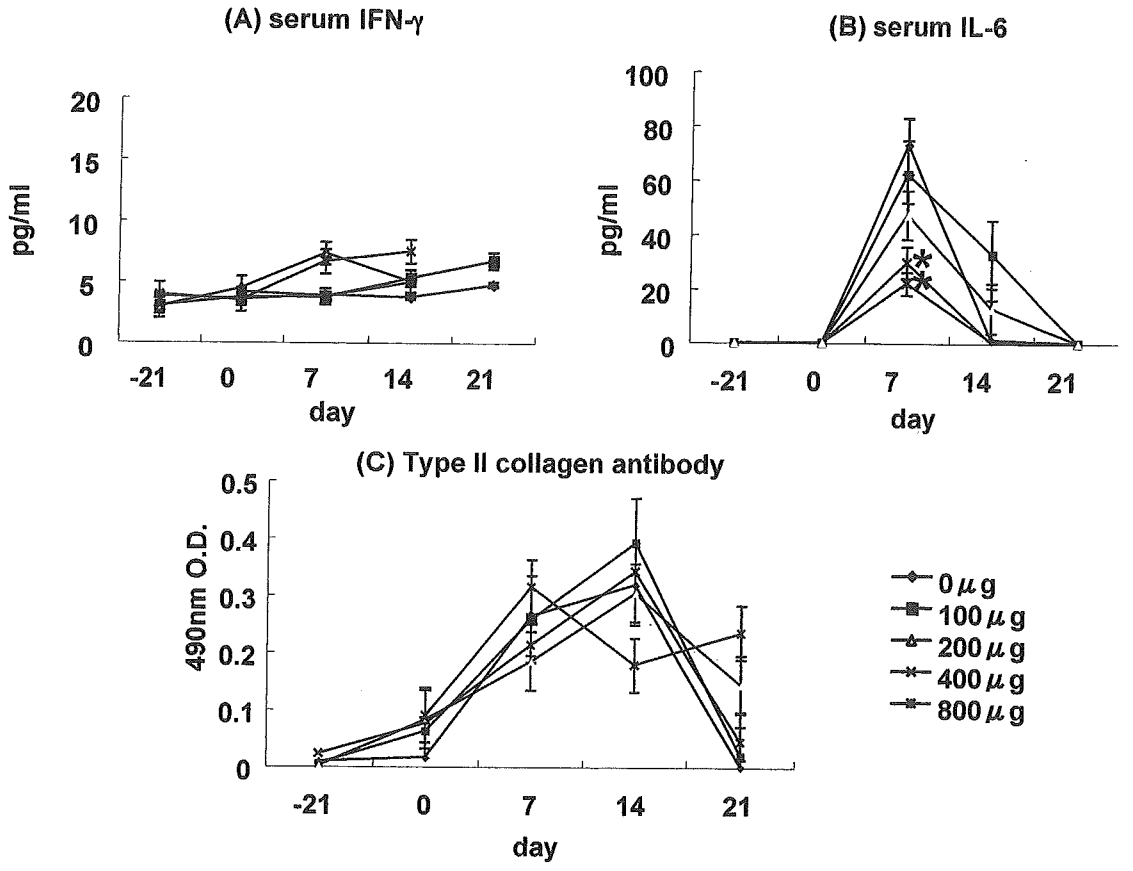

Figure 5. Effect of RXM treatment on serum levels of IFN-γ, IL-6, and type II collagen antibody in CIA mice, as described in Materials and Methods. Serum levels were plotted from 4 different doses of RXM (100, 200, 400, 800 μg; n = 8 for each group) and controls (n = 8). Mean values ± SD from 8 mice were plotted. IL-4 and TNF-α levels were always below background levels (data not shown). *$p < 0.05$, 0 versus 400 and 800 μg/day; 2-tailed Student t test.

duction by macrophages stimulated with LPS[31,32]. Recently, Guchelaar, *et al* reported that erythromycin inhibited TNF-α and IL-6 production induced by heat-killed *Streptococcus pneumoniae* in human whole blood *ex vivo*[33].

Systemic administration of macrolide antibiotics (erythromycin and RXM) has been shown to be effective in the treatment of lower and upper airway inflammatory diseases such as bronchial asthma and diffuse panbronchiolitis[2,32-34]. Although these inflammatory diseases have been reported to be successfully treated with low dose administration of macrolide antibiotics, which cannot be expected to act as antibacterial agents, the precise mechanisms of action to explain the clinical effectiveness of this therapy are not well understood. It was recently reported that bronchial asthma is a T cell-mediated inflammatory disorder, and selective recruitment of CD4+ T cells into sites of inflammation may contribute to the development of different pathological conditions[35,36]. Current studies suggest that TNF-α may potentially be involved in the development of bronchial hyperresponsiveness by directly altering the contractile properties of the airway smooth muscle[37,38]. As a regulator of IgE synthesis, increased levels of IL-6 have been detected in blood and bronchoalveolar lavage after bronchial challenge of patients with asthma, while bronchial biopsies of these patients reveal increased expression of IL-6[39]. Thus, inhibition of TNF-α and IL-6 production by T cells and macrophages as well as inhibition of T cell migration by RXM may also have important therapeutic implications for bronchial asthma.

In both CIA and RA, joint inflammation and cartilage and bone destruction depend on the concentrations of TNF-α and IL-6 in affected joints[28,40]. At the site of inflammation in the affected RA synovium, infiltration of leukocytes, especially T cells from blood vessels, is the initial step necessary for the development of the RA lesion. The *in vivo* effectiveness of RXM in preventing CIA development is likely linked to the ability of RXM to inhibit T cell migration and proinflammatory cytokine production by T cells and macrophages *in vitro*.

Based on the pharmacokinetics data in rats, oral administration of RXM at 5 mg/kg, which corresponds to 100 μg/mouse, resulted in the maximum plasma concentration around 1.9 μg/ml (2.3 μM). The usual dose in humans, 300 mg/adult, resulted in the maximum plasma concentration

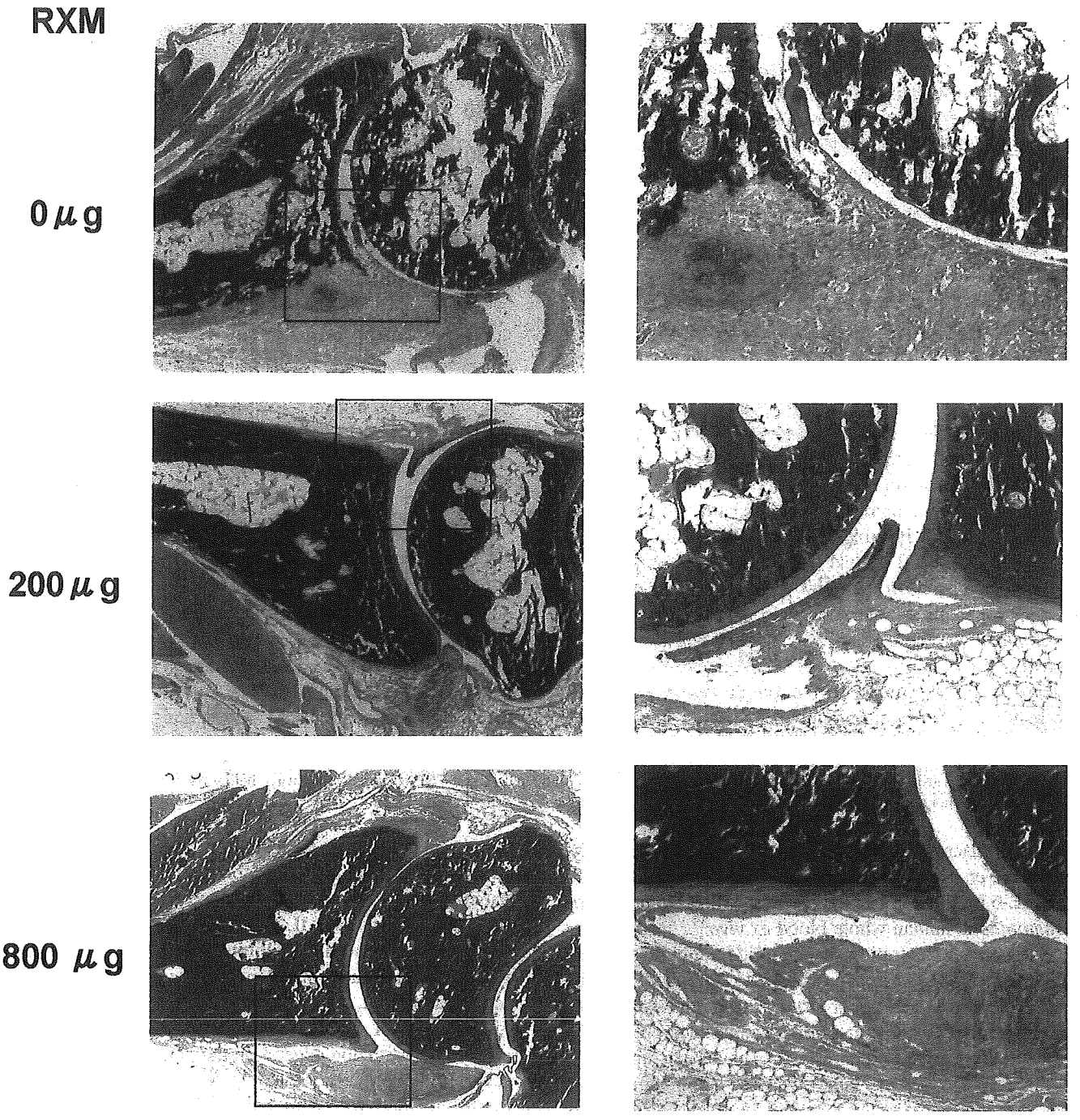

Figure 6. Ankle joints of CIA mice were collected on Day 21 after the second immunization of collagen. Mice had been treated with 0, 200, and 800 μg RXM. H&E stain; original magnification ×40 (left panels) and ×100 (right panels).

around 8.1 μg/ml (9.6 μM). Therefore, the *in vivo* concentration of RXM may correspond to the concentration that inhibits immune/inflammatory phenomena *in vitro*. Further, the doses employed in our *in vitro* and *in vivo* experiments correspond to the human daily dose.

Advances in understanding the pathogenesis of RA based on studies of human tissues and animal models of disease have led to identification of molecular targets for immunotherapeutic intervention. Of these, TNF-α has been validated as an appropriate target for treatment, and to date 2 biological agents that target TNF-α have been licensed for clinical use[40]. These are infliximab, an anti-TNF-α Mab[41], and etanercept, an engineered p75 TNF receptor dimer linked to the Fc portion of human IgG1[42]. Therapies inhibiting TNF-α in patients with active RA result in rapid and sustained improvement in symptoms and signs of disease, improve-

ment in the quality of life, and protection of joints from structural damage[40,43]. Moreover, anti-TNF-α treatment has been reported to be effective in Crohn's disease[44]. IL-6 regulates the production of acute-phase proteins by hepatocytes and activates osteoclasts to absorb bone[45,46]. In a preclinical study, a humanized anti-IL-6R Mab has been used to treat patients with severe RA, and clinical improvements have been reported[47].

Besides bronchial asthma, RA, and Crohn's disease, RXM may also be useful for the treatment of disorders in which TNF-α and IL-6 may play a role in pathophysiology, such as graft versus host disease (GVHD) following allogeneic bone marrow transplant[48], heart failure[49], and Castleman's disease[50].

ACKNOWLEDGMENT

The authors thank Fumiki Nojima for excellent secretarial assistance.

REFERENCES

1. Nelson S, Summer WR, Terry PB, Warr GA, Jakab GJ. Erythromycin-induced suppression of pulmonary antibacterial defenses. A potential mechanism of superinfection. Am Rev Respir Dis 1987;136:1207-12.
2. Kadota J, Sakito O, Kohno S, et al. A mechanism of erythromycin treatment on patients with diffuse panbronchiolitis. Am Rev Respir Dis 1993;147:153-9.
3. Miyatake H, Suzuki K, Taki F, Takagi K, Satake T. Effect of erythromycin on bronchial hyperresponsiveness in patients with bronchial asthma. Arzneimittelforschung 1991;41:552-6.
4. Yokota T, Suzuki E, Arai K. Cefpodoxime proxetil, its in vitro antibacterial activity, affinity to bacterial penicillin-binding proteins, and synergy of bactericidal activity with serum complement and mouse-cultured macrophages. Drugs Exp Clin Res 1988;14:495-500.
5. Fraschini F, Scaglione F, Ferrara F, Marelli O, Braga PC, Teodori F. Evaluation of the immunostimulating activity of erythromycin in man. Chemotherapy 1986;32:286-90.
6. Mikasa K, Sawaki M, Konishi M, et al. The effect of erythromycin treatment on natural killer cell activity in patients with chronic lower respiratory tract infections. Kansenshogaku Zasshi 1989;63:811-5.
7. Ras GJ, Anderson R, Eftychis HA, et al. Chemoprophylaxis with erythromycin stearate or amoxycillin in patients with chronic bronchitis — effects on cellular and humoral immune functions. S Afr Med J 1984;66:955-8.
8. Aho P, Mannisto PT. Effects of two erythromycins, doxycycline and phenoxymethylpenicillin, on human leucocyte chemotaxis in vitro. J Antimicrob Chemother 1988;21:29-32.
9. Anderson R. Erythromycin and roxithromycin potentiate human neutrophil locomotion in vitro by inhibition of leukoattractant-activated superoxide generation and autooxidation. J Infect Dis 1989;159:966-73.
10. Yoshimura T, Kurita C, Yamazaki F, et al. Effect of roxithromycin on proliferation of peripheral blood mononuclear cells and production of lipopolysaccharide-induced cytokines. Biol Pharm Bull 1995;18:876-81.
11. Young RA, Gonzalez JP, Sorkin EM. Roxithromycin. A review of its antibacterial activity, pharmacokinetic properties and clinical efficacy. Drugs 1989;37:8-41.
12. Noma T, Hayashi M, Yoshizawa I, Aoki K, Shikishima Y, Kawano Y. A comparative investigation of the restorative effects of roxithromycin on neutrophil activities. Int J Immunopharmacol 1998;20:615-24.
13. Wakita H, Tokura Y, Furukawa F, Takigawa M. The macrolide antibiotic roxithromycin suppresses IFN-gamma-mediated immunological functions of cultured normal human keratinocytes. Biol Pharm Bull 1996;19:224-7.
14. Konno S, Adachi M, Asano K, Okamoto K, Takahashi T. Inhibition of human T-lymphocyte activation by macrolide antibiotic roxithromycin. Life Sci 1992;51:L231-6.
15. Konno S, Asano K, Kurokawa M, Ikeda K, Okamoto K, Adachi M. Antiasthmatic activity of a macrolide antibiotic, roxithromycin: analysis of possible mechanisms in vitro and in vivo. Int Arch Allergy Immunol 1994;105:308-16.
16. Robey E, Allison JP. T-cell activation: integration of signals from the antigen receptor and costimulatory molecules. Immunol Today 1995;16:306-10.
17. Green JM, Noel PJ, Sperling AI, et al. Absence of B-7 dependent responses in CD28-deficient mice. Immunity 1994;1:501-8.
18. Gimmi CD, Freeman GJ, Gribben JG, et al. B-cell surface antigen B7 provides a costimulatory signal that induces T cells to proliferate and secrete interleukin 2. Proc Natl Acad Sci USA 1991;88:6575-9.
19. Morimoto C, Torimoto Y, Levinson G, et al. 1F7, a novel cell surface molecule, involved in helper function of CD4 cells. J Immunol 1989;143:3430-9.
20. Dang NH, Torimoto Y, Deusch K, Schlossman SF, Morimoto C. Comitogenic effect of solid-phase immobilized anti-1F7 on human CD4 T cell activation via CD3 and CD2 pathways. J Immunol 1990;144:4092-100.
21. Tanaka T, Kameoka J, Yaron A, Schlossman SF, Morimoto C. The costimulatory activity of the CD26 antigen requires dipeptidyl peptidase IV enzymatic activity. Proc Natl Acad Sci USA 1993;90:4586-90.
22. Hafler DA, Fox DA, Manning ME, Schlossman SF, Reinherz EL, Weiner HL. In vivo activated T lymphocytes in the peripheral blood and cerebrospinal fluid of patients with multiple sclerosis. N Engl J Med 1985;312:1405-11.
23. Iwata S, Yamaguchi N, Munakata Y, et al. CD26/dipeptidyl peptidase IV differentially regulates the chemotaxis of T cells and monocytes toward RANTES: possible mechanism for the switch from innate to acquired immune response. Int Immunol 1999;11:417-26.
24. Rosloniec EF, Cremer M, Kang A, Myers LK. Collagen-induced arthritis. In: Coligan JE, Kruisbeek AM, Margulies DH, Shevach EM, Strober W, editors. Current protocols in immunology. New York: Wiley; 1996:15.5.1-24.
25. Kapsenberg ML, Wierenga EA, Bos JD, Jansen HM. Functional subsets of allergen-reactive human CD4+ T cells. Immunol Today 1991;12:392-5.
26. Romagnani S. Lymphokine production by human T cells in disease states. Annu Rev Immunol 1994;12:227-57.
27. Johnston RB Jr. Current concepts: immunology. Monocytes and macrophages. N Engl J Med 1988;318:747-52.
28. Marinova-Mutafchieva L, Williams RO, Mason LJ, Mauri C, Feldmann M, Maini RN. Dynamics of proinflammatory cytokine expression in the joints of mice with collagen-induced arthritis. Clin Exp Immunol 1997;107:507-12.
29. Asano K, Kamakazu K, Hisamitsu T, Suzaki H. Modulation of Th2 type cytokine production from human peripheral blood leukocytes by a macrolide antibiotic, roxithromycin, in vitro. Int Immunopharmacol 2001;11:1913-21.
30. Morikawa K, Zhang J, Nonaka M, Morikawa S. Modulatory effect of macrolide antibiotics on the Th1- and Th2-type cytokine production. Int J Antimicrob Agents 2002;19:53-9.
31. Suzaki H, Asano K, Ohki S, Kanai K, Mizutani T, Hisamitsu T.

Suppressive activity of a macrolide antibiotic, roxithromycin, on pro-inflammatory cytokine production in vitro and in vivo. Mediators Inflamm 1999;8:199-204.
32. Iino Y, Toriyama M, Kudo K, Natori Y, Yuo A. Erythromycin inhibition of lipopolysaccharide-stimulated tumor necrosis factor alpha production by human monocytes in vitro. Ann Otol Rhinol Laryngol Suppl 1992;157:16-20.
33. Guchelaar HJ, Schultz MJ, van der Poll T, Koopmans RP. Pharmacokinetic-pharmacodynamic modeling of the inhibitory effect of erythromycin on tumour necrosis factor-alpha and interleukin-6 production. Fundam Clin Pharmacol 2002;15:419-24.
34. Itkin IH, Menzel ML. Pharmacokinetic-pharmacodynamic modeling of the inhibitory effect of erythromycin on tumour necrosis factor-alpha and interleukin-6 production. J Allergy 1970;45:146-62.
35. Robinson DS, Hamid Q, Ying S, et al. Predominant TH2-like bronchoalveolar T-lymphocyte population in atopic asthma. N Engl J Med 1992;326:298-304.
36. Ying S, Humbert M, Barkans J, et al. Expression of IL-4 and IL-5 mRNA and protein product by CD4+ and CD8+ T cells, eosinophils, and mast cells in bronchial biopsies obtained from atopic and nonatopic (intrinsic) asthmatics. J Immunol 1997;158:3539-44.
37. Baeuerle PA, Henkel T. Function and activation of NF-kappa B in the immune system. Annu Rev Immunol 1994;12:141-79.
38. Amrani Y, Chen H, Panettieri RA Jr. Activation of tumor necrosis factor receptor 1 in airway smooth muscle: a potential pathway that modulates bronchial hyper-responsiveness in asthma? Respir Res 2000;1:49-53.
39. Hirano T. Interleukin 6 and its receptor: ten years later. Int Rev Immunol 1998;16:249-84.
40. Harris ED Jr. Rheumatoid arthritis. Pathophysiology and implications for therapy. N Engl J Med 1990;322:1277-89.
41. Knight DM, Trinh H, Le J, et al. Construction and initial characterization of a mouse-human chimeric anti-TNF antibody. Mol Immunol 1993;30:1443-53.
42. Weinblatt ME, Kremer JM, Bankhurst AD, et al. A trial of etanercept, a recombinant tumor necrosis factor receptor:Fc fusion protein, in patients with rheumatoid arthritis receiving methotrexate. N Engl J Med 1999;340:253-9.
43. Lipsky PE, van der Heijde DM, St. Clair EW, et al. Infliximab and methotrexate in the treatment of rheumatoid arthritis. Anti-Tumor Necrosis Factor Trial in Rheumatoid Arthritis with Concomitant Therapy Study Group. N Engl J Med 2000;343:1594-602.
44. Kam LY, Targan SR. TNF-alpha antagonists for the treatment of Crohn's disease. Expert Opin Pharmacother 2000;1:615-22.
45. Castell JV, Gomez-Lechon MJ, David M, Hirano T, Kishimoto T, Heinrich PC. Recombinant human interleukin-6 (IL-6/BSF-2/HSF) regulates the synthesis of acute phase proteins in human hepatocytes. FEBS Lett 1988;232:347-50.
46. Tamura T, Udagawa N, Takahashi N, et al. Soluble interleukin-6 receptor triggers osteoclast formation by interleukin 6. Proc Natl Acad Sci USA 1993;90:11924-8.
47. Yoshizaki K, Nishimoto N, Mihara M, Kishimoto T. Therapy of rheumatoid arthritis by blocking IL-6 signal transduction with a humanized anti-IL-6 receptor antibody. Springer Semin Immunopathol 1998;20:247-59.
48. Jacobsohn DA. Novel therapeutics for the treatment of graft-versus-host disease. Expert Opin Investig Drugs 2002;11:1271-80.
49. Negrusz-Kawecka, M. The role of TNF-alpha in the etiopathogenesis of heart failure. Pol Merkuriusz Lek 2002;12:69-72.
50. Katsume A, Saito H, Yamada Y, et al. Anti-interleukin 6 (IL-6) receptor antibody suppress Castleman's disease-like symptoms emerged in IL-6 transgenic mice. Cytokine 2002;21:304-11.

Nonpathogenic *Escherichia coli* Strain Nissle1917 Prevents Murine Acute and Chronic Colitis

Nobuhiko Kamada, MS, Nagamu Inoue, MD, PhD,* Tadakazu Hisamatsu, MD, PhD,* Susumu Okamoto, MD, PhD,* Katsuyoshi Matsuoka, MD, PhD,* Toshiro Sato, MD, PhD,* Hiroshi Chinen, MD,* Kyong Su Hong, PhD,† Takaya Yamada, PhD,‡ Yumiko Suzuki, PhD,‡ Tatsuo Suzuki, PhD,‡ Noriaki Watanabe, MD, PhD,§ Kanji Tsuchimoto, MD, PhD,§ and Toshifumi Hibi, MD, PhD**

Background: Nonpathogenic *Escherichia coli* strain Nissle1917 has been used as a probiotics in human inflammatory bowel disease; however, there are few reports examining its therapeutic effect on animal colitis models, and its therapeutic mechanisms remain unknown. The aim of this study was to elucidate the therapeutic effect and mechanism of Nissle1917 using murine acute and chronic colitis models.

Methods: Two models were used. (1) Acute model: colitis was induced by administration of 1.3% dextran sodium sulfate for 7 days. Nissle1917 or phosphate-buffered saline were orally administered for 10 days. Mice were killed at day 10, and the colonic lesions were assessed macro- and microscopically. (2) Chronic model: IL-$10^{-/-}$ mice were treated with Nissle1917 or phosphate-buffered saline for 8 weeks. After 8 weeks of treatment, mice were killed to assess the colonic lesions macro- and microscopically. In the acute dextran sodium sulfate colitis model, viable, heat-killed, or genomic DNA of Nissle1917 was orally administered for 10 days, and the therapeutic effect was assessed.

Results: In the acute model, Nissle1917 ameliorated body weight loss, disease activity index, and macro- and microscopic damage. In the chronic model, it also suppressed the mucosal inflammatory findings and histologic damages. Moreover, heat-killed Nissle1917 or its genomic DNA alone also ameliorated the acute DSS colitis and viable bacteria macro- and microscopically.

Conclusions: Nonpathogenic *E. coli* strain Nissle1917 prevents both acute and chronic colitis, and its anti-inflammatory effect is exhibited not only by viable bacteria but also by heat-killed bacteria or its DNA.

Key Words: dextran sodium sulfate colitis, IL-10–deficient mouse, inflammatory bowel disease, Nissle1917, probiotics

(*Inflamm Bowel Dis* 2005;11:455–463)

Although the etiology of inflammatory bowel disease (IBD) remains unclear, a role for gut flora in the initiation and the perpetuation of IBD has been proposed. There is a possibility that an agent that is normally nonpathogenic, including a component of the normal gut flora, may be pathogenic in the susceptible host.[1] This hypothesis is supported by the observation that IBD is often improved by administration of antibiotics.[2] Studies of experimental colitis in various animal models have also shown the importance of the resident luminal flora in the initiation and the perpetuation of intestinal inflammation. The spontaneous colitis model, such as *T-cell receptor* α*-chain* gene–deficient mouse,[3,4] *interleukin-10* (*IL-10*) gene–deficient mouse,[5] *IL-2* gene–deficient mouse,[6] and *HLA-B27* gene transgenic rat,[7] requires the luminal bacteria for development of colitis. These genetically engineered rodents do not develop intestinal inflammation under germ-free conditions.

Probiotics are defined as living nonpathogenic organisms that confer health benefits by improving the microbial balance. Recently, it has been reported that probiotics are effective for treatment of IBD.[8–13] Nonpathogenic *Escherichia coli* strain Nissle1917 is one of the probiotic bacteria. This strain has no pathogenic potential besides the ability to colonize within the intestine. The results of a recent clinical trial showed that treatment with Nissle1917 is equivalent to mesalazine in maintaining remission of ulcerative colitis.[10,11] However, in animal experimental colitis models, there are few reports about the therapeutic effect of Nissle1917, and its mechanism of action remains unknown.

Received for publication June 20, 2004; accepted January 25, 2005.

From the *Department of Internal Medicine, School of Medicine, Keio University, Tokyo, Japan; †Research Center, Research Division, JCR Pharmaceuticals Co., Ltd., Kobe, Japan; ‡Division of BioMedical Research, BioMedical Laboratory, Kitasato Institute Hospital, Tokyo, Japan; and §Department of Internal Medicine, Kitasato Institute Hospital, Tokyo, Japan.

Supported by grants from JCR Pharmaceuticals Co., Ltd. (Kobe, Japan).

Reprints: Toshifumi Hibi, MD, Department of Internal Medicine, School of Medicine, Keio University, 35 Shinano-machi, Shinjuku-ku, Tokyo 160-8582, Japan (e-mail: thibi@sc.itc.keio.ac.jp)

This study aimed to estimate the therapeutic effect of Nissle1917 on murine acute and chronic colitis models and to elucidate its mechanisms of action.

MATERIALS AND METHODS

Animals

Specific pathogen-free female C57BL/6 mice, 6 to 7 weeks of age, were obtained from Clea Japan (Tokyo, Japan). Mice were housed less than 3 per cage at the animal center of Kitasato Institute Hospital (Tokyo, Japan) for 1 week before initiating the study. *IL-10* gene–deficient mice, generated on a C57BL/6 background, were obtained from Dr. Hiroshi Kiyono (Osaka University, Osaka, Japan) and were housed under conventional conditions at Keio University (Tokyo, Japan).

Preparation of Bacteria

The *E. coli* strain Nissle1917 (Mutaflor; DMS6601, serotype O6:K5:H1) was kindly supplied by Ardeypharm (Herdecke, Germany). It was expanded from freeze stock to a Luria-Bertani (LB) agar plate and grown for 24 hours at 37 °C. Colonies on LB agar plates were collected and suspended in sterile phosphate-buffered saline (PBS, pH 7.4). Concentration was determined by photometric comparison with a previously established growth curve. Bacterial suspension was prepared in 5×10^8 colony forming units (CFUs) per milliliter. Heat-killed bacteria were prepared by resuspending viable bacteria in PBS followed by incubation for 30 minutes at 60 °C. Killed bacteria were washed and resuspended in PBS. The complete killing was confirmed with 24-hour incubation at 37 °C on an LB agar plate. Genomic DNA was isolated from Nissle1917 using the Genomic DNA isolation kit (Qiagen Sciences, Valencia, Calif.).

Genomic Polymerase Chain Reaction of Nissle1917

Female C57BL/6 mice (8 wk of age) were orally administered *E. coli* Nissle1917. One to 10 days after administration, stools were collected and cultured in LB medium overnight at 37 °C. Bacterial genomic DNA was extracted from the cultured medium using QIA amp DNA Stool Mini Kit (Qiagen Sciences). Genomic polymerase chain reaction (PCR) for Nissle1917 was performed as previously described.[14] Briefly, *E. coli fimB* gene primers were forward, 5′-GGCGTCGACTAACCCAGCACAG-CTA-3′, and reverse, 5′-GCGCGGATCCGTAAGAATAATGT-AGT-3′. For genomic PCR, equivalent amounts of genomic DNA (1 μL), 10× PCR buffer, 1.25 mM dNTPs, 0.5 U recombinant Taq polymerase (Takara, Tokyo, Japan), and 0.5 μM of the forward and the reverse primers were used. Cycling conditions for PCR amplification were 94 °C for 5 minutes and 40 cycles of 94 °C for 30 seconds, 55 °C for 30 seconds, and 72 °C for 30 seconds, followed by a final extension at 72 °C for 7 minutes.

Nissle1917 Treatment in a Murine Acute Colitis Model

Each group of mice was fed 1.3% dextran sulfate sodium (DSS; molecular weight 50,000; BioResearch Corp., Yokohama, Japan) for 7 days. All groups of mice were orally administered with Nissle1917 (1×10^8 CFU/mouse/d) or PBS for 10 days. In other experiments, heat-killed Nissle1917 (1×10^8 CFU/mouse/d) and Nissle1917 genomic DNA (10 μg/mouse/d) were administered in the same manner. In all mice, body weight and disease activity index (DAI) were assessed on a daily basis. DAI was determined by a scoring system as previously described.[15] Briefly, the index is as follows: loss of body weight—0 = none, 1 = 1% to 5%, 2 = 5% to 10%, 3 = 10% to 20%, 4 = >20%; stool consistency—0 = normal stool, 2 = loose stool, 4 = diarrhea; hemoccult—0 = normal, 2 = hemoccult positive, 4 = gross blood. DAI is the sum of the 3 scores divided by 3. Mice were killed at day 10, and the resected colonic tissue was examined macroscopically and microscopically. For cytokine analysis, mice were killed at day 7 and purified lamina propria mononuclear cells (LPMCs) were examined.

Nissle1917 Treatment in a Murine Chronic Colitis Model

Eight-week-old IL-$10^{-/-}$ mice were orally administered Nissle1917 (1×10^8 CFU/mouse/d) or PBS for 8 weeks. The disease activity of colitis was determined in the same way as the experiments for the acute colitis model.

Histologic Score

Mice were killed at each period. Colons were harvested and fixed in 10% phosphate-buffered formalin. These samples were paraffin-embedded, sectioned, and stained with hematoxylin and eosin. Tissues were reviewed in a blinded fashion and assessed with a previously validated gastrointestinal histologic inflammatory score. (1) For DSS colitis mice,[16] histologic scores ranged from 0 to 12. Total score was assessed as the sum of the following 4 parameters: extent, 0 to 3 [0, none; 1, focal; 2, limited to 1 segment (proximal, middle, distal); 3, involving more than 1 segment]; inflammation, 0 to 3 (0, none; 1, mild; 2, moderate; 3, severe); damage/necrosis, 0 to 3 (0, none; 1, mild; 2, moderate; 3, severe); and regeneration, 0 to 3 (0, complete re-epithelialization; 1, broad or multifocal re-epithelialization; 2, focal migration and mitotic features; 3, none). (2) For IL-$10^{-/-}$ mice,[17] histologic scores ranged from 0 to 10. Total score was assessed as the sum of the following 4 parameters: mucosal ulceration, 0 to 3 (0, normal; 1, surface epithelial inflammation; 2, erosions; 3, ulcerations); epithelial hyperplasia, 0 to 3 (0, normal; 1, mild; 2, moderate; 3, pseudopolyps); lamina propria mononuclear infiltrate, 0 to 2 (0, normal; 1, slightly increased; 2, markedly increased); and lamina propria neutrophil infiltrate, 0 to 2 (0, normal; 1, slightly increased; 2, markedly increased).

Enzyme-linked Immunosorbent Assays for Serum Amyloid A

Blood samples were collected, and the serum fraction was separated. Serum was analyzed for serum amyloid A (SAA) protein by enzyme-linked immunosorbent assay kit (BioSource International, Calif.). Basal SAA protein levels were obtained from age-matched wild-type control mice. The cut-off value was calculated as mean + 2 SD of wild-type control SAA concentrations.

Isolation of LPMCs

Mice were killed, and colonic tissues were removed. Removed colons were washed with calcium- and magnesium-free Hanks balanced salt solution (HBSS; Sigma, St. Louis, Mo.) and dissected into small pieces. The tissues were incubated in HBSS containing 2.5% fetal bovine serum (BioSource) and 1 mM dithiothreitol (Sigma) to remove mucus. They were incubated twice in HBSS containing 1 mM EDTA (Sigma) for 20 minutes at 37 °C. Then they were washed with HBSS for 3 times and incubated in HBSS with 1 mM collagenase type IV (Sigma) for 2 hours at 37 °C. The digested tissues were filtered and washed twice with HBSS. Cells were resuspended in 40% Percoll (Pharmacia Biotech, Piscataway, NJ) and layered on the 75% Percoll before centrifugation at 2000 rpm for 20 minutes. Cells recovered from the interphase were washed twice and suspended in HBSS. Cell viability was >95%, as determined by trypan blue exclusion dye.

Analysis of Proinflammatory Cytokines Expression by Quantitative Reverse Transcription-PCR

Total RNA was isolated from LPMCs using RNeasy Mini kit (Qiagen Sciences). cDNA was synthesized from 1 μg total RNA with Omniscript reverse transcriptase (RT; Qiagen Sciences). For quantitative RT-PCR, equivalent amounts of cDNA (2 μL), 0.5 μM of the forward and reverse primers, and DyNAmo SYBR Green qPCR Kit (MJ Research, Waltham, Mass.) were used. The PCR reactions were carried out in a thermocycler DNA engine, OPTICON2 (MJ Research). Cycling conditions for PCR amplification were 95 °C for 10 minutes, and 40 cycles of 95 °C for 10 seconds and 58 °C for 50 seconds. Murine-specific primers for tumor necrosis factor (TNF)-α were forward, 5′-CATCTTCTCAAAATTCGAGTGACAA-3′, and reverse, 5′-TGGGAGTAGACAAGGTACAACCC-3′. Interferon (IFN)-γ primers were forward, 5′-TCAAGTGGCATAGATG-TGGAAGAA-3′, and reverse, 5′-TCACCATCCTTTTGCC-AGTTCCTCCAG-3′. IL-1β primers were forward, 5′-CAACCAACAAGTGATATTCTCCATG-3′, and reverse, 5′-GATCCACACTCTCCAGCTGCA-3′. IL-6 primers were forward, 5′-GAGGATACCACTCCCAACAGACC-3′, and reverse, 5′-AAGTGCATCATCGTTGTTCATACA-3′. Transforming growth factor (TGF)-β1 primers were forward, 5′-TGACGT-CACTGGAGTTGTACGG-3′, and reverse, 5′-GGTTCATGT-CATGGATGGTGC-3′. Monocyte chemoattractant protein (MCP)-1 primers were forward, 5′-CTTCTGGGCCTGC-TGTTCA-3′, and reverse, 5′-CAAGCCTACTCATTGG-GATCA-3′. Macrophage inflammatory protein (MIP)-2 primers were forward, 5′-ATCCAGAGCTTGAGTGTGACGC-3′, and reverse, 5′-AAGGCAAACTTTTTGACCGCC-3′. IL-10 primers were forward, 5′-GGTTGCCAAGCCTTATCGGA-3′, and reverse, 5′-ACCTGCTCCACTGCCTTGCT-3′. β-actin primers were forward, 5′-AGAGGGAAATCGTGCGTGAC-3′, and reverse, 5′-CAATAGTGATGACCTGGCCGT-3′.

Statistical Analysis

All data are expressed as mean ± SEM. Differences between means were evaluated using Mann-Whitney *U* test for analysis.

RESULTS

Nissle1917 Ameliorates Murine DSS Colitis

To identify the mechanisms of action of Nissle1917 in murine acute colitis models, we first examined the effect of Nissle1917 in the DSS colitis model. To detect the *Nissle1917* gene from murine fecal samples, we generated primers to amplify a specific insert in the *fimB* gene in Nissle1917 (Fig. 1A). As shown in Figure 1B, specific gene amplification of Nissle1917 in feces of mice could be detected only on day 1 after the single administration, which suggested the absence of its colonization. Because, in this detection system, primers could amplify the other *E. coli fimB* gene in a competitive manner, the smaller product from the other *E. coli* may be amplified easier than Nissle1917. Therefore, these data may

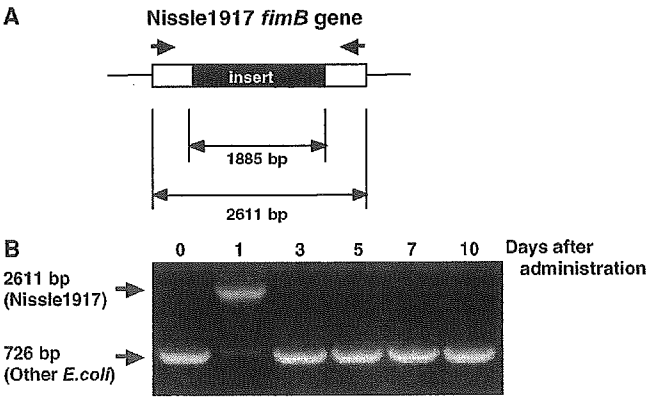

FIGURE 1. Detection of Nissle1917 from murine fecal samples. A, the set of primers was designed to amplify the sequence containing the specific insert element located in the *fimB* gene of Nissle1917. B, detection of Nissle1917 from murine fecal samples by PCR. Nissle1917 (1×10^8 CFU/mouse) was orally administrated into C57BL/6 mice. Nissle1917-specific amplified products were detected only 1 day after administration.

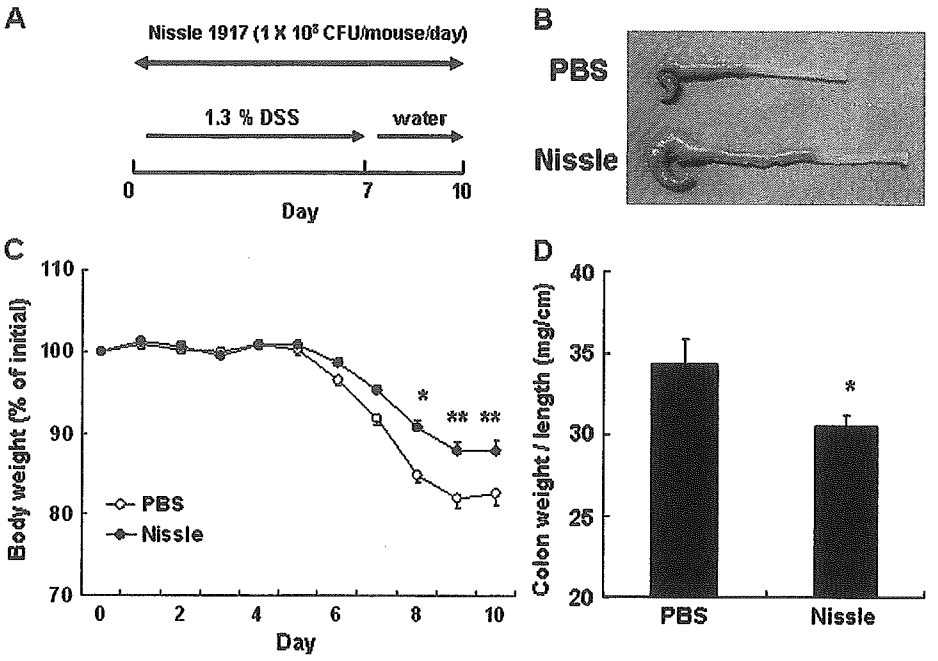

FIGURE 2. Effect of Nissle1917 on DSS-induced colitis. A, protocols for induction of DSS colitis. B, macroscopic findings of the colons from DSS colitis mice treated with PBS (top) or Nissle1917 (bottom). C, body weight losses of mice treated with PBS (○, n = 36) or Nissle1917 (●, n = 34). D, colon weights of DSS colitis mice treated with PBS (n = 10) or Nissle1917 (n = 10). Results are expressed as mean ± SEM *, $P < 0.05$; **, $P < 0.01$ compared with PBS groups.

not show the complete disappearance of orally administrated Nissle1917. In this study, we administered Nissle1917 for 10 consecutive days to make sure of its sufficient presence and examined the therapeutic effect (Fig. 2A). Macroscopic findings revealed that the shortening and thickening of the colon were improved in the Nissle1917 group (Fig. 2B). The body weight started to decline 6 days after the intake of DSS in both control and Nissle1917 groups. However, after day 8, the body weight loss was significantly reduced in the Nissle1917-treated group (Fig. 2C; control: 84.9 ± 1.0% versus Nissle: 90.6 ± 0.9%; $P < 0.05$ at day 8, control: 82.0 ± 1.1% versus Nissle: 87.8 ± 1.1%; $P < 0.01$ at day 9, and control: 82.6 ± 1.3% versus Nissle: 87.8 ± 1.2%; $P < 0.01$ at day 10). Consistent with the results of body weight, DAI scores and colon weight (control: 34.3 ± 1.5 versus 30.5 ± 0.8 mg/cm; $P < 0.05$ at day 10) were also lower in the Nissle1917 group (Fig. 2D; Table 1). Neither healthy controls nor the Nissle1917 group without DSS administration showed any body weight loss or macroscopic sign of colitis (data not shown). Colons from DSS-induced colitis mice treated with PBS contained severe ulceration and inflammatory cell infiltration over the proximal and distal region (Fig. 3C). In contrast, DSS colitis mice treated with Nissle1917 showed significantly less inflammation and ulceration (Fig. 3D). On the other hand, Nissle1917 itself did not affect normal colonic mucosa (Fig. 3B). Histologic scores were also reduced in the Nissle1917 group (Fig. 3E; control: 10.7 ± 0.3 versus Nissle: 8.2 ± 0.5; $P < 0.05$). Thus, we considered that Nissle1917 provided protective effect on colonic mucosa in murine acute colitis.

Nissle1917 Reduces Chronic Colonic Inflammation in IL-10$^{-/-}$ Mice

We next examined whether Nissle1917 was also effective against chronic colonic inflammation. We used IL-10$^{-/-}$ mice as a model of chronic colonic inflammation, as previously described.[18] IL-10$^{-/-}$ mice developed spontaneous enterocolitis associated with body weight loss, passage of mucus, rectal prolapse, and diarrhea. In this experimental period, there was no significant alteration in body weight in each group (data not shown). Colon weights of IL-10$^{-/-}$ mice were increased after the development of inflammation, but Nissle1917

TABLE 1. DAI Scores of DSS-induced Colitis Mice

	PBS (N = 36)	Nissle (N = 34)
Day 1	0.05 ± 0.02	0.04 ± 0.02
Day 2	0.15 ± 0.04	0.09 ± 0.03
Day 3	0.22 ± 0.04	0.15 ± 0.03
Day 4	0.42 ± 0.06	0.31 ± 0.07
Day 5	0.79 ± 0.10	0.49 ± 0.06
Day 6	1.47 ± 0.13	0.87 ± 0.11†
Day 7	2.32 ± 0.13	1.31 ± 0.14‡
Day 8	2.62 ± 0.10	1.73 ± 0.12‡
Day 9	2.47 ± 0.08	1.81 ± 0.15†
Day 10	2.23 ± 0.12	1.69 ± 0.13*

Data are mean ± SEM.
*$P < 0.05$, †$P < 0.01$, and ‡$P < 0.0001$, significant difference from PBS group.

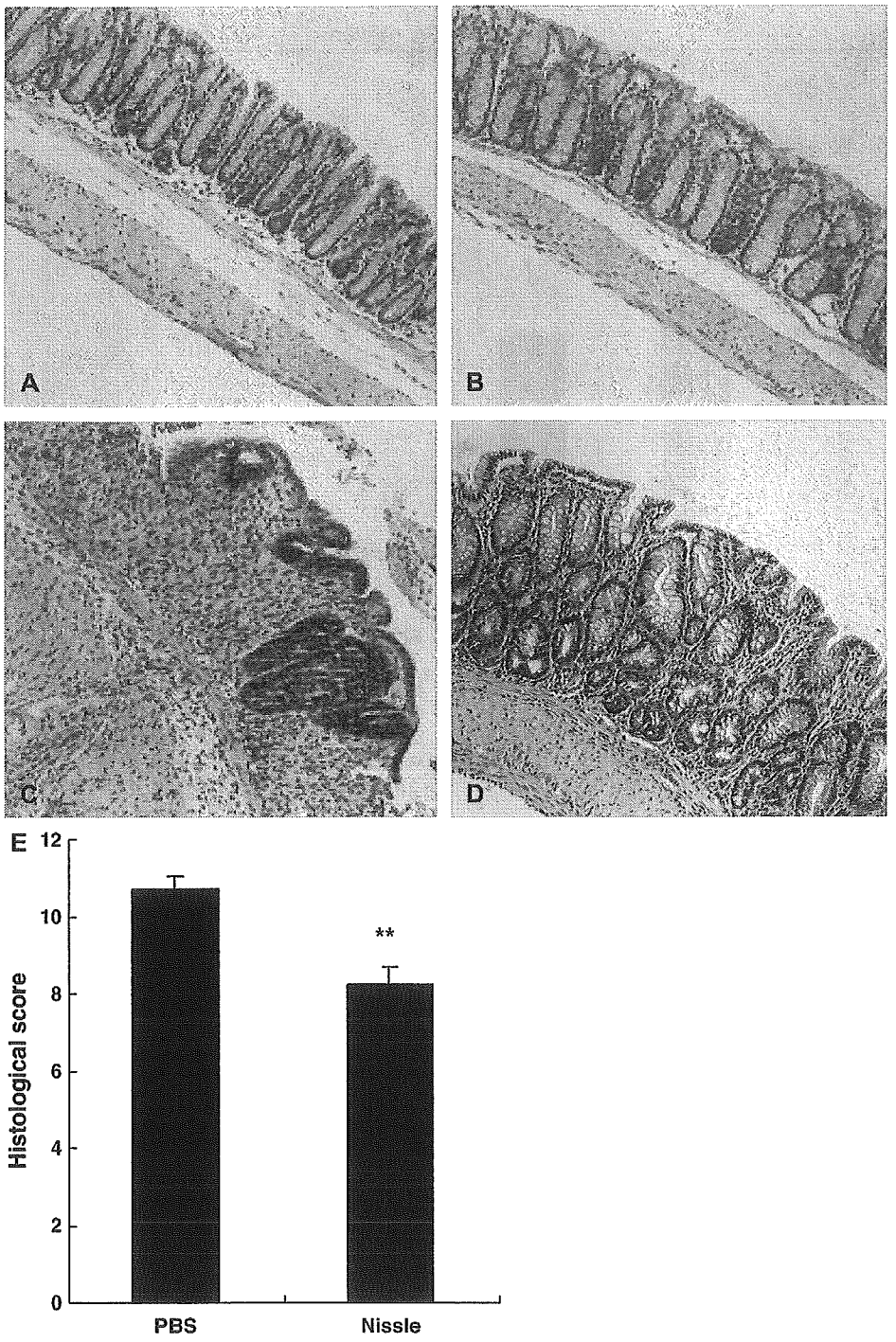

FIGURE 3. Histologic findings of the colonic tissues from DSS colitis mice treated with Nissle1917. A, normal colon. B, colon of mice treated with Nissle1917. C, DSS-induced colitis treated with PBS (day 10). D, DSS-induced colitis treated with Nissle1917. E, histologic scores of DSS-induced colitis mice (n = 11, PBS group; n = 10, Nissle group). Results are expressed as mean ± SEM of the data from 3 independent experiments. **, $P < 0.01$ compared with PBS groups.

treatment decreased this inflammatory findings (Fig. 4A and B; control: 52.3 ± 2.4 versus Nissle: 50.0 ± 1.5 mg/cm; $P < 0.05$). The number of mice with rectal prolapse, 1 of the characteristic symptoms of severe rectal inflammation, was significantly decreased in the Nissle1917 group (Fig. 4C; control: 5.6% at 3 wk after administration and 16.7% at 7 wk after administration, Nissle: 0% in the experimental periods).

The SAA protein concentrations, which can be a useful marker of inflammation, were significantly lower in Nissle1917-treated mice (229.5 ± 93.7 μg/mL) than in control mice (47.0 ± 17.8 μg/mL; Fig. 4D; $P < 0.01$). Microscopically, marked infiltrations of mononuclear cells and polymorphonuclear cells were observed in colonic mucosa of control IL-$10^{-/-}$ mice (Fig. 5A). In contrast, Nissle1917-treated mice

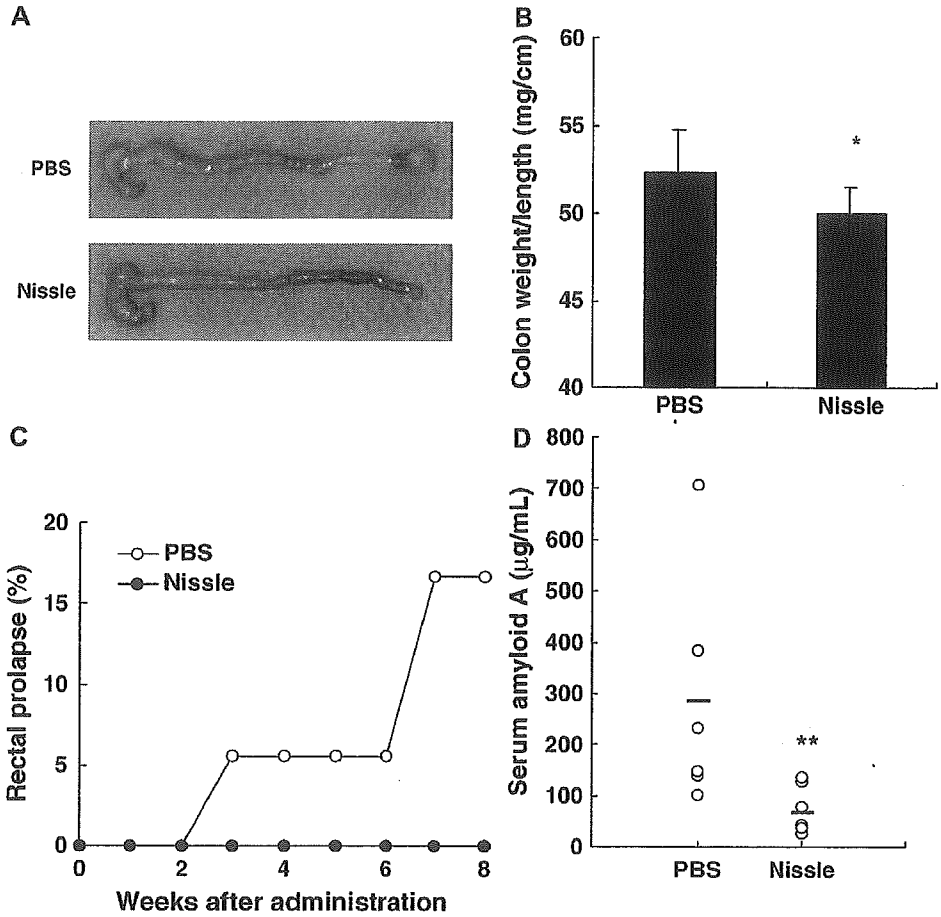

FIGURE 4. Effect of Nissle1917 on IL-$10^{-/-}$ mice. A, macroscopic findings of IL-$10^{-/-}$ murine colon treated with PBS (top) or Nissle1917 (bottom). B, colon weights of IL-$10^{-/-}$ mice treated with PBS (n = 18) or Nissle1917 (n = 17). C, rectal prolapse of IL-$10^{-/-}$ mice treated with PBS (○, n = 18) or Nissle1917 (●, n = 17). D, SAA protein levels of IL-$10^{-/-}$ mice treated with PBS (n = 6) or Nissle1917 (n = 7). Results are expressed as mean ± SEM of the data from 3 independent experiments. *, $P < 0.05$; **, $P < 0.01$ compared with PBS groups.

showed significantly less infiltrations of these cells (Fig. 5B). Histologic scores were also significantly reduced in Nissle1917-treated mice (Fig. 5C; control: 5.2 ± 0.6 versus Nissle: 3.6 ± 0.5; $P < 0.05$).

Nissle1917 Suppresses the Expression of Proinflammatory Cytokines and Chemokines in LPMCs

Because the mechanisms of the protective effect of Nissle1917 on murine colonic inflammation remain unknown, we next examined the expression of several proinflammatory cytokines and chemokines in LPMCs isolated from DSS colitis mice and IL-$10^{-/-}$ mice with or without Nissle1917 treatment. Quantitative RT-PCR for TNF-α, IFN-γ, IL-1β, IL-6, TGF-β1, IL-10, MCP-1, and MIP-2 were performed. As shown in Figure 6, mRNA expression of most cytokines and chemokines tested were not significantly reduced in DSS colitis mice. However, in IL-$10^{-/-}$ mice, IFN-γ and MIP-2 expressions were significantly lower in Nissle1917-treated mice than those in controls (IFN-γ, control: 100 ± 9.9% versus Nissle: 62.7 ± 14.2% and MIP-2, control: 100 ± 22.8% versus Nissle: 31.8 ± 10.1%; $P < 0.05$).

Heat-killed and Genomic DNA from Nissle1917 Ameliorates Murine DSS Colitis

To prove the therapeutic mechanism of Nissle1917, the efficacy of nonviable Nissle1917 components on experimental colitis was assessed. In DSS colitis mice, macroscopic findings revealed that the shortening and thickening of the colon were significantly improved in all Nissle groups compared with the PBS control group (Table 2). Histologic findings also showed less inflammation in all Nissle groups, and the histologic scores of these groups were significantly lower than controls (Table 2). In terms of DAI scores at day 7, heat-killed Nissle1917 and genomic DNA treatment diminished the scores, but the difference was not statistically significant against untreated mice. However, in earlier phase of DSS colitis, genomic DNA treatment clearly suppressed the inflammation with reduced DAI score (control: 0.9 ± 0.2 versus DNA: 0.4 ± 0.2; $P < 0.05$ at day 5, control: 1.8 ± 0.2 versus DNA: 1.0 ± 0.2; $P < 0.05$ at day 6).

DISCUSSION

Probiotic bacteria have been used on human clinical disorders including IBD. For example, probiotic VSL#3 (comprised